SYNTHESIS AND CHARACTERISATION OF GOLD-IODINE NANOCOMPOSITE SUPPORTED ON HONEY AND EVALUATION OF ITS DELIVERY ON OPEN WOUND TREATMENT

BY

LAWAL, Mohammed Adavize MTech/SPS/2018/8129

DEPARTMENT OF CHEMISTRY

SCHOOL OF PHYSICAL SCIENCES

FEDERAL UNIVERSITY OF TECHNOLOGY MINNA

OCTOBER, 2023

SYNTHESIS AND CHARACTERISATION OF GOLD-IODINE NANOCOMPOSITE SUPPORTED ON HONEY AND EVALUATION OF ITS DELIVERY ON OPEN WOUND TREATMENT

BY

LAWAL, Mohammed Adavize MTech/SPS/2018/8129

A THESIS SUBMITTED TO THE POSTGRADUATE SCHOOL FEDERAL UNIVERSITY OF TECHNOLOGY, MINNA, NIGER STATE, NIGERIA IN **PARTIAL FULFILMENT OF THE REQUIREMENTS FOR THE AWARD OF THE MASTERS DEGREE IN CHEMISTRY (ANALYTICAL CHEMISTRY)**

OCTOBER, 2023

DECLARATION

I, **LAWAL, Mohammed Adavize** hereby declare that this thesis titled: "**Synthesis and Characterisation of Gold-Iodine Nanocomposite Supported on Honey and Evaluation of its Delivery on open Wound Treatment**" is a collection of my original research work under the supervision of late Dr. (Mrs) M.T Bankole and Dr. J.O Tijani. And it has not been presented for any other qualification elsewhere, by anybody in any form. Information from other sources (published or unpublished) and all citation has been duly acknowledged in the work by way of reference.

LAWAL, MOHAMMED ADAVIZE _____

MTECH/SPS/2018/8129 SIGNATURE/DATE

FEDERAL UNIVERSITY OF TECHNOLOGY MINNA

NIGER STATE, NIGERIA

CERTIFICATION

The thesis titled **"Synthesis and Characterisation of Gold-Iodine Nanocomposite Supported on Honey and Evaluation of its Delivery on Open Wound Treatment"** by: LAWAL, Mohammed Adavize (MTech/SPS/2018/8129) meets the regulations governing the award of degree of (Masters Degree) of the Federal University of Technology, Minna and it is approved for its contribution to scientific knowledge and literary presentation.

DR. J. O. TIJANI _____

MAJOR SUPERVISOR SIGNATURE & DATE

DR. (MRS) L. A. FADIPE _____

HEAD OF DEPARTMENT SIGNATURE & DATE

PROF. M. JIYA
DEAN OF SCHOOL OF PHYSICAL SCIENCES _____ SIGNATURE & DATE

ENGR. PROF. O. K. ABUBAKRE _____

DEAN OF POSTGRADUATE SCHOOL SIGNATURE & DATE

DEDICATION

This project work is dedicated to Almighty God and also to the loving memory of my late supervisor Dr. (Mrs). M.T Bankole (Iyaayiayo) who went to meet the Lord in the course of this project.

ACKNOWLEDGEMENTS

I wish to express my profound gratitude to Almighty God for giving me the strength to wade through this phase of my life, without his unfailing love, today would have been impossible. My special thanks and gratitude to my able supervisors: Late Dr. (Mrs). M.T Bankole and Assoc. Prof. J.O Tijani, for their dedication, guidance and mentorship on this work. It has been a good experience working under your tutelage. May Almighty God bless and reward you for your constructive criticism geared towards the success of this project work.

My appreciation goes to Assoc. Prof (Mrs) L. A. Fadipe (H.O.D), Prof. M.A.T Suleiman,

Prof. J. Yisa, Prof. Y. A. Iyaka, Prof. A. Mann, Prof. S.S. Ochigbo, Prof. M. M. Ndamitso,

Prof. J.O. Jacob, Prof. A.I. Ajai, Mr, M.T Bisiriyu, Mrs. Z. Abdullahi, Mr. E.Y. Shaba, Miss N. Nwakife, Miss A. Andrew and other members of staff of the Department of Chemistry

for their encouragement and assistance rendered during the course of this study. God bless you
all.

I sincerely appreciate Dr. (Mrs). R. Lafia-Araga (Co-ordinator of Postgraduate Studies, Department of Chemistry) for all her efforts in making sure that the program is coherent and also instilling moral and professional values in us the students. May God bless you mama. Also, my sincere appreciation goes to the entire Laboratory Technologists of the Department of Chemistry and other lecturers of various departments. Not forgetting Prof. A. S. Abdulkareem and Dr. Saheed Mustapha who in one time or the other impacted knowledge in me. May God Almighty bless you and be with you all.

To my dear parents and loving siblings, I appreciate your love, prayers, support and advice. And my supportive friends, I sincerely appreciate your efforts. May God guide and protect us all.

My special overwhelming gratitude to Mr Aminu-Bello Dange, Mr Daniel Ipaye, Miss Majeedah Adekanbi, Mrs Sakina Ahmed and Mr Kayode Ologuntere. Thank you all for your support, may Almighty God grant all your heart desires.
Similarly, to my wonderful friends and course mate who supported in one way or the other.

Worthy of mention are Sarah Udenyi Onugwu, Linda Uselegh, Usman Nurudeen Ayodeji, Haruna Hajarat Ozozoma, John Paul and others. Thank you for everything and may God bless you and grant your desires.

ABSTRACT

This study focuses on the development and application of Au-Iodine nanocomposite (AuINCs) and Au-Iodine/honey nanocomposite (Au-I/honeyNCs) for drug delivery on resistance bacteria in open wound treatment. In this research gold nanoparticles (AuNPs) were synthesized using green method via reduction of gold chloride, by *Agerantum conyzoides* leaves extract. The synthesized colloidal AuNPs was modified with povidone iodine and honey using wet impregnation and ultra-sonication methods. The gold-ioidne nanocomposite and gold-iodine-honey composite were characterized using UV- Vis spectroscopy, High Resolution Transmission Electron Microscope (HRTEM), Selected Area Electron Diffraction (SAED), and Energy Dispersive Spectroscopy (EDS). The

UVvisible analysis confirmed the appearance of a broad peak at 548 nm for AuNPs and 536 nm for both gold-iodine nanocomposite and Au/Iodine/Honey composite. The HRTEM micrograph revealed well dispersion of triangle, octahedral, and icosahedral AuNPs, Auiodine and Auiodine/honey nanocomposite with an average particle size of 13.08, 32.60 and 37.57 nm respectively. The EDX showed Au, I and carbon as the dominant elements in the composite sample. The SAED indicated the formation of crystalline AuNPs, amorphous Au-iodine nanocomposite and partly crystalline Au-iodine/honey nanocomposite having face centered cubic structure of Au. The narrow size distribution and the absence of agglomeration suggest that pure honey matrix prevent the agglomeration of gold-iodine nanocomposite. In-vitro release of Au-iodine nanocomposite and Au-iodine/honey nanocomposite was studied using dialysis bag method on certain strains of bacteria. After 180min reaction time, Au-INCs has a cumulative maximum concentration release 73.57%, 68.72% and 67.07% on *Staphylococcus aureus, E.coli* and *Pseudomonas aeruginosa* respectively. While AuI/honeyNCs has cumulative maximum concentration release of 99.54%, 96.91%, 97.62% on *Staphylococcus aureus, E.coli* and *Pseudomonas aeruginosa*. The release kinetic model for Au-INCs and Au-I/honeyNCs is best fit to Zero order model while the magnitude of release on *Staphylococcus aureus* followed fickian diffusion and non-fickian diffusion for *E.coli* and *Pseudomonas aeruginosa.* In-vitro release demonstrated gold-iodine-honey composites as viable therapeutic agents for open wound treatment compared to the gold nanoparticles alone.

TABLE OF CONTENTS

CHAPTER ONE
1

CHAPTER TWO
7

LIST OF TABLES

LIST OF FIGURES

LIST OF PLATES

LIST OF ABBREVIATIONS

EDS	Energy Dispersive X-ray Spectrum
EMB	Eosin Methylene Blue Agar
HRTEM	High Resolution Transmission Electron Microscopy
SAED	Selected Area of Electron Distribution
UV/VISIBLE	Ultra Violet Visible Spectroscopy

CHAPTER ONE

1.0 INTRODUCTION

1.1 Background to the study

Human skin offers protection to muscles, bones, ligaments and internal organs against microbes (Eshgh *et al*., 2022). It helps to regulate body temperature, permits the sensations of touch, heat and cold as well as act as an immune system to the human body (Wang *et al*., 2019). There are three primary layers of skin which are epidermis, dermis and hypodermis (Kim *et al*., 2019). Of these three, the epidermis, which is the outer layer is prone to several factors like abrasion, cuts, laceration and could result to different types of skin damage and wound (Kumar *et al*., 2022). Wounds are referred to as the breakage or disruption of the skin caused by trauma or medical/physiological condition, thereby damaging the anatomical structure and ultimately result to the loss of skin physiological function (Patra *et al*., 2018). Wounds can be chronic or acute in nature. For instance, acute wounds usually occur as a result of mechanical damage or exposure to extreme heat, electrical shock, irradiation or corrosive chemicals (Hernández-Rangel and Martin-Martinez, 2021). Such wounds heal within a short period of time if correct wound management is applied (Nethi *et al*., 2019). Chronic wounds are complication of some specific diseases like diabetes ulcer, which has horrific effect (Nethi *et al*., 2019). These wounds take longer time to heal and can reoccur at extremely high rate unless the root disease is cured (Patra *et al*., 2018).

The wound healing process is often thwarted by some multi-antibiotic resistant bacteria in wound such as *Staphylococcus aureus, Pseudomonas aeruginosa* and *Escherichia coli* (Sadat *et al*., 2022). These bacteria have the ability to form resistance against conventional drugs thereby causing deleterious infections on wounds (Sadat *et al*., 2022). These infections

are harder to treat, leading to higher medical cost, prolonged hospital stay and increased mortality (Noorbakhsh *et al*., 2021). Hence, there is a need to develop novel drug of high therapeutic efficacy against these bacteria and non-toxic delivery vehicle that will excellently control the release of drugs to their target-site within short period of time.

Since time immemorial, human have widely used natural-based products such as plants and pure honey as medicine against various diseases including wound healing (Napagoda and Witharana, 2020). Many plant's part such as fruits, seeds, oil, leaves, bark and roots play an important role in the healing of wounds and also reveals significant role in diseases prevention due to their rich source of antioxidants (Napagoda and Witharana, 2020).

Examples of such plants are: *Azadirachta indica, Ageratum conyzoides, Carica papaya, Euphorbia heterophylla, Jatropha curcas, Ocimum gratissimum* and *Sida acuta.*

Honey is a natural product formed from nectar of flowers by honeybees (*Apismellifera*; Family: *Apidae*) (Toledo-Hernandez *et al*., 2022). Honey has been used by humans since ancient times, most ancient population, including the Greeks, Chinese, Egyptians, Romans, Mayans, and Babylonians, consumed honey both for nutritional aims and for its medicinal properties (Patouna *et al*., 2023). Honey is the only insect-derived natural product that has nutritional, cosmetic, therapeutic, and industrial values (Abbas *et al*., 2021). Evidence indicates that honey can exert several health-beneficial effects including antioxidant antiinflammatory, antibacterial, antidiabetic, respiratory, gastrointestinal, cardiovascular and nervous system protective effects (Abbas *et al*., 2021). Despite the use of these naturalbased products, infection and microbial implantation are factors that have posed threat to chronic wound healing (Kolimi *et al*., 2022).

Iodine is a widely used antiseptic and has been in use for more than a century for treatment of open wounds (Bigliardi *et al*., 2017). It has a wide spectrum of antimicrobial activity with efficacy against bacteria, mycobacteria, fungi, protozoa and viruses and can be used to treat both acute and chronic wounds (Gmur and Karpiński, 2020). It is also relatively inexpensive and easy to use, but is often underused as a topical antiseptic due to its perceived toxicity.

In recent time researches have been tailored towards employing nanomaterials for open wound treatment and drug delivery (Bukhari *et al*., 2021). Nanomaterials in the form of non-metal and metal possess different antimicrobial properties (Bukhari *et al*., 2021). Among the metallic nanoparticles, gold nanoparticles have been widely recognized due to it antibacterial activity and target delivery of active agents (Wang *et al*., 2019). The ability to carry, protect and sustain active drug release is a good advantage of gold nanomaterials over modernized dressings. Over the years several delivery vehicles were designed based on different nanomaterial such as polymer, nanotubes, dendrimers, liposomes, (Patra *et al*., 2018) to mention but few. However metallic nanoparticle such as gold nanoparticles have been proven as an attractive vehicle for drug delivery to their target sites (Chandrakala *et al*., 2022) due to its unique properties like high stability, high dispersity, easy to functionalize, non-cytotoxicity and biocompatibility (Patra *et al*., 2018). Nevertheless, information regarding gold nanoparticles as a vehicle for drug delivery on bacteria causing deleterious effect in open wound has not been reported. Thus, the present study focused on the synthesis, characterisation and application of gold-iodine nanocomposite (Au-INCs) and gold-iodine/honey nanocomposite (Au-I/honeyNCs) on certain strains of bacteria in open wound treatment.

1.2 Statement of the Research Problem

Wound treatment is still a major problem in developing countries despite earnest investigation to improve cutaneous wound care; clinical treatment of chronic wounds remains unsatisfactory in many cases. Globally, chronic wound is estimated at 1.51 per 1000 population (Martinengo *et al*., 2019). When a large sized active agent is dispersed on a wound bed it is rapidly absorbed or eliminated, which may lead to period of overexposure or underexposure. Thus, a little or over time is spent within the therapeutic range of the active agent which may result to prolong wound healing and wastage of the active agent (Bruschi, 2018). The use of large sized materials like macro-molecules as drug delivery vehicle constitute major challenges such as instability, poor bioavailability, solubility and absorption in the body, issues with target-specific delivery, extent of toxicity and probable adverse effect of drugs on open wound (Patra *et al*., 2018). Despite all the advantages of *Agerantum conyzoides* L, it wound healing efficiency is often retarded by certain strain of bacteria such as *Staphylococcus aureus*, *Pseudomonas aeruginosa* and *Escherichia coli* (Adelakun *et al*., 2018).

Although honey is cheap and readily available and possess wound healing properties but however, it has a slow release on wound bed thereby prolonging wound healing period (Jaldin *et al*., 2022). Low penetration of active agents in the open wound and local tissue reactions are some of the common problems encountered in the course of wound treatment. For instance, iodine-based agents in wound treatment, have been linked to allergy, excruciating pain, ineffective penetration and toxic effects on host cells (Bigliardi *et al*., 2017).

1.3 Justification of the Study

Nanosize gold particles plays a significant role in advanced drug formation, targeting arena with excellent control of drug release and delivery due to its unique properties like high stability, dispersity, easy to functionalize, non-cytotoxicity and biocompatibility (Patra *et al*., 2018). Thus, it is expected to shorten wound healing period and reduce the quantity of active agent used for wound care. Gold nanocomposite has been proven to possess capability to modify active agent properties like diffusivity and offer protection against proteases in wound (Kumar *et al*., 2019).

Bonding iodine with gold nanoparticles makes it less toxic and instead of high concentrations of iodine being released in a single application, the iodine is slowly released from the reservoir carrier molecule over a sustained period of time (Edis *et al*., 2019). Hence, its efficacy is enhanced within the therapeutic range (Bruschi, 2018). Gold-iodine nanocomposites supported on honey is expected to be effective against bacteria, fungi and virus in wounds thereby reducing the period of time required to heal with enhanced pharmacokinetic.

1.4 Aim and Objectives of the Study

The aim of this study is to synthesise gold/iodine nanocomposites supported on honey and evaluate its kinetic delivery on *Escherichia coli*, *Pseudomonas aeruginosa* and *Staphylococcus aureus* bacteria in wounds.

The above aim was achieved through the following specific objectives:

i. Screen for phytochemical constituent of *Agerantum conyzoides* leaf extract and natural honey.

ii. Synthesise gold nanoparticles (AuNPs) using *Agerantum conyzoides* leaf extract.

iii. Functionalization/modification of gold nanoparticles with iodine and natural honey via wet impregnation and sonication.

iv. Characterise synthesised gold nanoparticles and gold-iodine nanocomposites (AuI/NCs), gold-honey nanocomposite (Au-HoneyNCs) and gold-iodine/Honey nanocomposite (Au-I/HoneyNCs) using different analytical tools.

v. Evaluate uncontrolled delivery of iodine on *Staphylococcus aureus, Pseudomonas aeruginosa* and *Escherichia coli* using dialysis bag method.

vi. Evaluate *in-vitro* delivery of Au-I-NCs and Au-I/HoneyNCs on *Staphylococcus aureus, Pseudomonas aeruginosa* and *Escherichia coli* using dialysis bag method.

vii. Evaluate Au-I/HoneyNCs and Au-I/NCs released data using mathematical kinetic model (Zero order, first order, Higuchi model and Kosmeryer-peppas model).

CHAPTER TWO

2.0 LITERATURE REVIEW

2.1 Wounds

Wounds are defined as the breakage or disruption of skin caused by trauma or medical/physiological conditions. Under such circumstance, frequent damage to skin anatomical structure and the loss of skin physiological functions occur (Patra *et al*., 2018). The wounds generally fall into two categories: acute wounds often result from mechanical damage or exposure to extreme heat, irradiation, electrical shock or corrosive chemicals (Patra *et al*., 2018). Such wounds heal in a relatively short period of time if supported by appropriate wound management (Tottoli *et al*., 2020). Chronic wounds normally appear to be the complication of some specific diseases like diabetes, which is notorious for its horrendous incidence of ulcers (Tottoli *et al*., 2020). These wounds require longer time to heal and their reoccurrence rates are extremely high unless the root diseases are cured (Rayman *et al*., 2020). According to wound depth, the wounds can be classified as three kinds: superficial wounds (only lose a part of epidermis), partial thickness wounds (epidermis and deeper dermal layers are affected) and full thickness wounds (subcutaneous fat and deeper tissues are disrupted) (Sullivan and Myers, 2022).

2.2 Wound healing

Cutaneous wound healing consists of three partially overlapping phases: hemostasis and inflammation, new tissue formation, and tissue remodeling (plate I). Within these broad phases, there exist a series of tightly regulated event involving chemotaxis, phagocytosis, neocollagenesis, collagen degradation, and collagen remodeling (Sullivan and Myers, 2022). In addition, wound healing in human is a complicated biological process requiring the coordinated migration and proliferation of both keratinocytes and fibroblasts, as well as other

cell types to mount an inflammatory response, synthesize granulation tissue, and restore the epithelial layer (Wang *et al*., 2019).

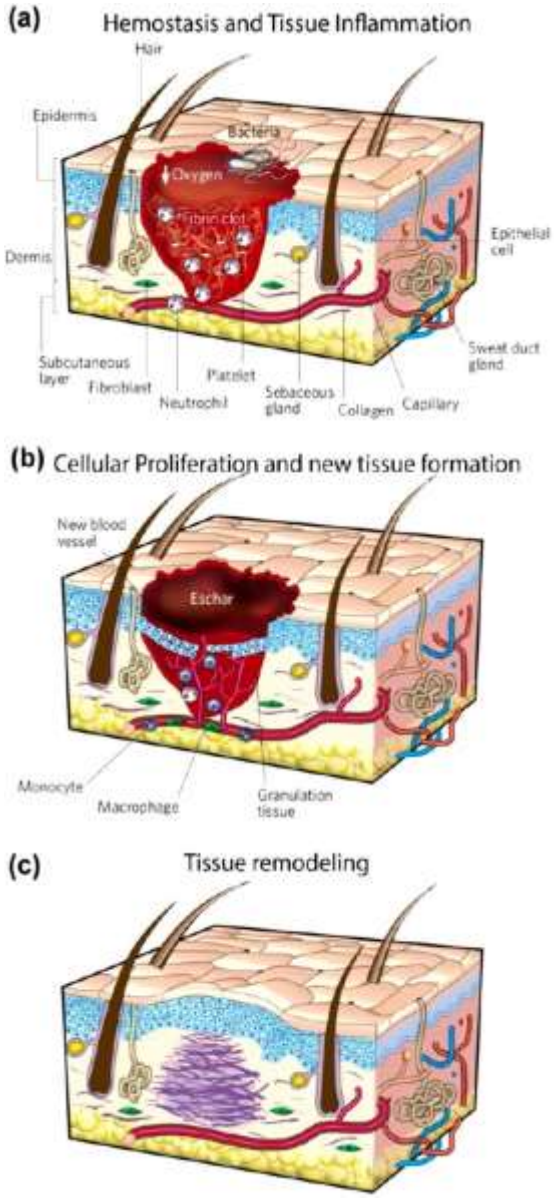

Plate I: Wound healing phases (Wang *et al*., 2019).

2.2.1 Hemostasis and tissue inflammation

The inflammatory phase often lasts 2 to 5 days after skin damage. When an injury occurs, the hemostasis is initiated immediately by intravascular platelets to form a clot and stop bleeding (Wang *et al*., 2019). Furthermore, platelets will be activated by thrombin and release several growth factors such as epidermal growth factor (EGF), insulin-like growth factor 1 (IGF-1), platelet-derived growth factor (PDGF), fibroblast growth factor (FGF), transforming growth factor (TGF-α and TGF-β) (Rahman *et al*., 2021). These growth factors diffuse into wound tissue and serve as biological signals to attract neutrophils, monocytes, leukocytes and macrophages, which will further mediate the inflammation, protect skin from infection and secret more growth factors to accelerate wound healing
(Wang *et al*., 2019).

2.2.2 Proliferative phase and new tissue formation

The proliferative phase generally takes 3 days to 2 weeks after injury and featured with cell proliferation and migration (Gomez *et al*., 2020). Fostered by proangiogenic factors such as PDGF released by platelets and inflammatory cells within wound area, new blood vessels and capillaries gradually take shape (Wang *et al*., 2019). Simultaneously with angiogenesis, migration of fibroblasts is also elicited by the stimulation of platelet-derived growth factor and fibroblast growth factor from inflammatory cells to form granulation tissue (Marofi *et al*., 2021). With the accumulation and proliferation of fibroblasts, new extracellular matrix composed of collagen, proteoglycans, and elastin is produced. Some fibroblasts even differentiate into myofibroblasts and play a role in the contraction of wound area (Marofi *et al*., 2021). Moreover, activated keratinocytes around wound margin migrate to injured area to complete re-epithelialization (Gomez *et al*., 2020).

2.2.3 Re-modeling phase

Re-epithelialization and remodeling phase varies from 3 weeks to 2 years post-injury. The collagen in newly synthesized ECM is gradually replaced by collagen I and the new born collagen fibers evolve into a more organized lattice structure, augmenting tensile strength of healed skin (Wang *et al*., 2019). The cells that had been used to repair the wound but which are no longer needed are removed by apoptosis, or programmed cell death. When collagen is laid down during the proliferative phase, it is disorganized and the wound is thick. During the maturation phase, collagen is aligned along tension lines and water is reabsorbed so the collagen fibers can lie closer together and cross-link. Cross-linking of collagen reduces scar thickness and also makes the skin area of the wound stronger.

Remodeling phase also concerns about scar formulation (Shoseyov *et al*., 2019).

2.3 Wound healing materials

Since times immemorial, human beings have widely used plant-based natural products as medicines against various diseases including wound healing. Modern medicines primarily derived from herbs based on traditional knowledge and practices are also used. About 25% of the major pharmaceutical compounds are obtained from natural resources (Enrico, 2019). Natural products having varieties of molecular backgrounds are used for the discovery of novel drugs for wound healing (Patra *et al*., 2018). These natural products possess extraordinary characteristic such as chemical diversity, chemical and biological properties with micromolecular specificity and less toxic making them favorable in the discovery of novel drugs for wound healing. It is believed that the plant extract is commonly used as a medicament for wounds and indigestion. However, natural compounds are now being screened for treating several major diseases, including cancer, diabetes, cardiovascular, inflammatory, and microbial diseases (Enrico, 2019). This is mainly because natural drugs

possess unique advantages, such as lower toxicity and side effects, cost effectiveness, and good therapeutic potential. However, concerns associated with the biocompatibility, and level of toxicity of natural compounds with respect to dosage portend a greater challenge of using them as medicine.

2.3.1 Plant (*Agerantum Conyzoides L*)

Agerantum conyzoides L. is an invasive plant belonging to the family Asteraceae. It has been used for the treatment of a wide range of diseases in various parts of Asia, Africa and South America (Chahal *et al*., 2021). It is frequently used as a purgative, febrifuge, antimicrobial, anti-ulcer, anti-inflammatory, anti-dysenteric, anti-lithic and wound dressing (Adesanwo *et al*., 2019). It is also used to treat diseases associated with bleeding, particularly wounds and burns (Adesanwo *et al*., 2019). *Agerantum conyzoides* has imparted numerous ethno medicinal uses because it has been used to cure ailments such as leprosy, skin disorder, sleeping sickness, rheumatism, headaches, dyspnea, toothache, pneumonia and many more (Adesanwo *et al*., 2019).

In this study, *Agerantum conyzoides L* known as goat weed commonly found in the environment which belongs to the family *Asteraceae* is a plant widely used for the treatment of diseases; as purgative, febrifuge, antimicrobial, anti−ulcer, anti-inflammatory and wound dressing (Sathyaseelan *et al*., 2020). It is also used to treat diseases associated with bleeding, particularly in the treatment of wounds and burns (Sathyaseelan *et al*., 2020).

A number of phytoconstituents have been screened such as alkaloids, flavonoids, terpenes, chromenes, and sterols from almost every part of this plant. These phytochemical constituents have shown diverse pharmacological properties including antimicrobial, antiinflammatory, analgesic, antioxidant, anticancer, antiprotozoal, antidiabetic,

spasmolytic, allelopathy, and many more (Chahal *et al*., 2021). This plant is found abundantly in and around agroecosystems and is considered an emerging invader. *Ageratum conyzoides L* can stop bleeding and accelerate healing process thereby improving healing percentage and the density of collagen fibers of hyperglycemic wound (Seyed and Ayesha, 2021). *Ageratum conyzoides* L. has many benefits; the leaves had been previously reported to contain secondary metabolites compounds such as alkaloids, tannins, phenols, saponin, and flavonoids (Seyed and Ayesha, 2021). *Ageratum conyzoides* leaves are traditionally used to cure pneumonia, cuts and sores, antidote to snake venom, anti-tetanus, headache, typhoid fever, uterine problems, malarial fever, throat infection, painful gums, and leucorrhoea (Chahal *et al*., 2021).

Stem **flower** **leaves**

Plate II: *Ageratum conyzoides* (a) Stem (b) Flower and (c) Leaves (Omotoso *et al*., 2019)

In the field of nanotechnology, plants remain the potential source to obtain various secondary active metabolites (Anjum *et al*., 2021). Using their extracts in biochemical synthesis of various nanomaterials, they possess important functional groups such as hydroxyl and carboxylic groups containing compounds, which could perform the role of reducing agent as well as stabilizing agent. However, in attempt to synthesize metallic nanoparticles that is free

of toxic by-product, the synthesis procedures need to be carried out under appropriate conditions in an aqueous medium and thus, its worthy to be considered as a green process.

Recently, researchers have centered on plant-oriented nanoparticle synthesis due to its numerous advantages over conventional synthesis methods (Mishra *et al*., 2021). For instance, Rana *et al*. (2020) revealed that plant reduction mechanism is a factor in controlling the size of nanomaterial as well as its stability. With respect to that, aqueous extract of plant materials is usually analysed quantitatively for their chemical constituents and phenolic compounds reported to be the most common metabolites present in all plants (Kisiriko *et al*., 2021). Plant extract is considered as a cost effective approach since its preparation involved the use of agro-waste such as leave, roots, fruit peels and flowers. These natural resources can be employed either as a fresh or dried materials. Both methods reduce cost, but they require days or hours to dry the plant materials completely. On the contrary, (Zhang *et al*., 2022) evidenced that samples dried with freeze-dryer was the preeminent method so as to preserve the content of reducing agents concurrently.

2.3.2 Honey

Honey is as a balanced diet and equally popular for male and female in all ages (Zanchini *et al*., 2022). Honey requires no refrigeration, it never spoils, and it can also be stored unopened at room temperature in a dry place (Dongare *et al*., 2019). The water activity (WA) of honey is between 0.56 and 0.62 and its value of pH is almost 3.9 (Dongare *et al*., 2019). Honey was utilized as a natural sweetener from ancient period since it has high level of fructose (honey is 25% sweeter than tablet sugar). Moreover, the use of honey in beverages is also increasingly popular (Starowicz *et al*., 2021). Nowadays, information on the usage of honey for the cure of many human diseases can be found in general magazines, journals, and

natural products' leaflets and suggesting a wide variety of unknown activities. Honey induces leukocytes to release cytokines, which is what begins the tissue repair cascades (Nezhad-Mokhtari *et al*., 2021).

2.3.3 Iodine

Iodine is a natural dark violet, non-metallic element that plays a key role in human metabolism (Alotaibi, 2021). It is essential for the production of thyroid hormones and an iodine deficiency can result in hypothyroidism. Iodine occurs naturally in the form of iodide ions in sea water, fish, oysters and certain seaweeds (Alotaibi, 2021). It can also be found in vegetables grown in iodinerich soil and dairy products. It has been described as 'the most potent antiseptic available (Alotaibi, 2021). Iodine is a highly effective topical antimicrobial that has been used clinically in the treatment of wounds for times immemorial (Rai *et al*., 2019). It has a wide spectrum of antimicrobial activity with efficacy against bacteria, mycobacteria, fungi, protozoa and viruses and can be used to treat both acute and chronic wounds (Gmur and Karpiński, 2020).

The antimicrobial properties of iodine were first demonstrated in 1882 by Davaine. In the First World War, iodine was found by Alexander Fleming to reduce the incidence of gas gangrene in the wounds of soldiers when compared to carbolic acid. It is also relatively inexpensive and easy to use, but is often underused as a topical antiseptic due to its perceived toxicity (Gmur and Karpiński, 2020). It has been suggested that iodine has a negative impact on cells involved in the wound healing process and because of this its safety and efficacy have been questioned (Davane *et al*., 2019). Iodine (as well as antiseptics in general) in wound treatment is believed to cause allergic reactions, to be less effective due to poor penetration, or to negatively influence tissue regeneration due to a toxic effect on the host cells (Bai *et al*., 2023). Bonding iodine with another molecule makes it less toxic and the iodine is slowly released from the reservoir carrier molecule over a sustained period of time (Davane *et al*., 2019). The two most commonly used iodophors in modern wound

dressings: Povidone iodine (PVP-I): a chemical complex of polyvinylpyrrolidone (also known as povidone and PVP) and elemental iodine. Examples include dressings such as Inadine (Systagenix) and solutions such as Betadine (Purdue Products) and Braunol (B Braun) and Cadexomer iodine: an iodine and polysaccharide complex, such as Iodoflex and Iodosorb, which can be used as antiseptic fillers, particularly in cavity wounds.

There is substantial *in vitro* evidence demonstrating that PVP-I is a highly effective and broad-spectrum antimicrobial (Gmur and Karpiński, 2020). Activity has been demonstrated against both common bacterial wound isolates and antibiotic-resistant species (Gmur and Karpiński, 2020).

2.4 Nanomaterials

The application of nanotechnology to the field of medicines and pharmaceuticals has revolutionized the twentieth century. Nanotechnology refers to a new field of science which includes synthesis and development of various nanomaterials (Mostafavi *et al*., 2019). Nano is a Greek word that means small in size and used as the prefix for the billionth from the range 9 to 10. Particles which have two or more dimensions in the size range as 1 to 100 nm are defined as nanoparticles (ASTM International) (Trotta and Mele, 2019). Nanoparticles have unique chemical and physical properties as compared to their solid bulk counterpart because of their high surface area and electronic properties (Saleh, 2020). Also, these particles have been utilized in electrochemistry, photochemical, and biomedicine (Soni *et al*., 2018). Nanoparticles have many functional platforms that can be utilized for imaging and therapeutic activities. These platforms can be prepared from various inorganic and organic materials, but the inorganic platforms are very essential for simultaneous therapy and diagnosis because of their easy modification, high drug loading capacity and stability (Lui *et*

al., 2022). Nanoparticles can be used in drug delivery and in the determination of drugs in pharmaceuticals (Wang *et al*., 2019). Currently, different metallic nanoparticles such as copper, zinc, titanium, magnesium, gold, alginate and silver are being produced. These nanoscale metals and their oxides have been widely used in environmental mitigation and wastewater treatment (Aragaw *et al.*, 2021). Even today various disease like diabetes, cancer, Parkinson's disease, Alzheimer's disease, cardiovascular diseases and multiple sclerosis as well as different kinds of serious inflammatory or infectious diseases (e.g. HIV) constitute a high number of serious and complex illnesses which are posing a major problem for the mankind. Nano-medicine makes use of nano materials, and nano electronic biosensors. In the future, nano medicine will benefit molecular nanotechnology. The medical area of nano science application has many projected benefits and is potentially valuable for all human races (Wang *et al*., 2019). With the help of nano medicine early detection and prevention, improved diagnosis, proper treatment and follow-up of diseases is possible. Certain nano scale particles are used as tags and labels, biological can be performed quickly, the testing has become more sensitive and more flexible. With the help of nanotechnology, damaged tissue can be reproduced or repaired. These so called artificially stimulated cells are used in tissue engineering, which might revolutionize the transplantation of organs or artificial implants.

2.4.1 Gold nanoparticles

Gold nanoparticles are widely used in biotechnology and biomedical field because of their large surface area, and high electron conductivity (Asiya *et al*., 2020). The modification of the nanometers is done to increase the interaction of these nanoparticles with biological cells (Gholipourmalekabadi *et al*., 2017). Enhanced permeability and retention are the unique property of nanoparticles to accumulate and interact with the tumor cells (Herdiana *et al*.,

2021). Drug delivery systems depend on nanoparticles, which are used in targeting malignant brain tumors where the conventional therapy is not as much effective (Garanti *et al*., 2021). The gold nanoparticles have been proven to be the safest and much less toxic agents for drug delivery (Yafout *et al*., 2021). Nanoparticles such as dendrimers, quantum dots, polymer gels, and gold nanoparticles have more properties and widely used in some application such as drug delivery systems and imaging (Kumar *et al*., 2020). Inorganic nanoparticles are widely used as a contrast agent in some application, especially molecular imaging such as computed tomography, positron emission tomography, magnetic resonance imaging, optical imaging, and ultrasound (Siddique and Chow, 2020). In addition, there are some applications of gold nanoparticles in electrochemistry involving the determination of Pharmaceutical compounds. It is commonly used in the electrochemical methods because of its ease of fabrication, better sensitivity determination and modification surface. AuNPs are proper for some surface immobilization, acting as conducting materials and enhancing the electron transfer between the surface of gold nanoparticles and the target analyte (Siddique and Chow, 2020). Gold nanoparticles have many applications, such as catalysis, optical molecular sensing, cancer therapeutics, and construction blocks in nanotechnology (Yafout *et al*., 2021). The applicability of gold nanoparticles in drug delivery systems is due to have some of the properties to make it good vehicle property for drug delivery. Fabrication of gold nanoparticles can perform to have a different size from 1 nm to 150 nm (Bharadwaj *et al*., 2021). Their structural design enables the coating of the surfaces with various targeting agents. In addition, the important properties are non-toxic and biocompatible (Wang *et al*., 2019). The gold nanoparticles have good physical, chemical and optical properties and photo properties of gold nanoparticles can be innovative ways to control the transport pharmaceutical compounds and control (Hammami and Alabdallah, 2021). Their structural

design enables the coating of the surfaces with various targeting agents. In addition, the important properties are non-toxic and biocompatible (Hammami and Alabdallah, 2021).

2.4.2 Synthesis of gold nanoparticle

The fabrication of AuNPs with distinct sizes, shapes and decorations with different functionalities make them a fascinating platform for drug-delivery systems. AuNPs can be synthesized by the reduction of gold salts in the presence of stabilizing agent in order to prevent agglomeration. Various methods have been employed to synthesize gold nanoparticles (Hammami and Alabdallah, 2021). The techniques used for the preparation of nanoparticles involved biological, physical, and chemical methods.

2.4.3 Chemical method

This method often requires chemical reaction during the synthesis of AuNPs in the presence of reducing agent and/or stabilizing agents such as sodium citrate, heparin, hyaluronan, ascorbic acid and sodium borohydride (Li *et al*., 2017). This method involves the reduction process of the $HAuCl_4$ through a solution of thiolated chitosan (Gulati *et al*., 2021). Thermal citrate reduction method can also be used in the preparation of AuNPs via

Raman spectroscopy using inositol hexakisphosphate (IP_6) to reduce $HAuCl_4$ (El-Kheir and El-Gabry, 2022). In addition, the preparation of Au/NPs may be by the trisodium citrate, and hydrogen tetrachlorocuprate (III) tetrahydrate (chloroauric acid) (El-Kheir and ElGabry, 2022). Gold nanoparticles are prepared by utilizing peptide-biphenyl hybrids

(PBHs) as a stabilizer for gold, and in this method the size range 1.8 to 3.7 nm was reported (Gulati *et al*., 2021). The dendrimers/Au nanoparticles can be prepared by the reduction of a solution of $HAuCl_4$ and sodium borohydride (Li *et al*., 2017).

2.4.4 Physical method

The gamma-irradiation technique is one approach for the synthesis of AuNPs with uniform size from the range 5-40 nm and high purity, using polysaccharide alginate as stabilizer (Hassan *et al*., 2022). The microwave irradiation technique was used to prepare AuNPs by reducing agents such as citric acid and a binding agent such as cetyltrimethylammonium bromide (CTAB) (Hassan *et al*., 2022). Furthermore, AuNPs are prepared using heat or photochemical reduction, and reduction of $HAuCl_4$ by citrate, tartrate, and malate (Hassan *et al*., 2022). A common method of photochemical reduction has been recorded for the synthesis of gold-polyethylene glycol nanoparticles by polymerization reactions with size 10-50 nm. Furthermore, in this approach, gold salt is reduced by radical formation coated with polyethylene glycol diacrylate by UV-reaction Hassan *et al*., 2022).

2.4.5 Biological method

This method involves the use of bacteria or fungi as a source to produce AuNPs, avoiding the use of organic solvents. This method is more environmental benign compared to chemical and physical methods for the production of AuNPs (Lee *et al*., 2020). Fathil *et al*., (2022) reported the production of AuNPs in which Au precursor were dissolved in NaCl solution from the bulk gold substrate using natural chitosan without any stabilizer and reductant. Another green synthesis method of Au/NPs with size from 15-80 nm was reported by (Shittu *et al*., 2017). In this approach, $HAuCl_4$ was used as a precursor and reduced by utilizing citrus fruit juice extracts (*Citrus limon*, *Citrus reticulate* and *Citrus sinensis*). Recently green synthesis of AuNPs using plant extract has been developed, where the extract themselves simultaneously act as stabilizing and reducing agents for AuNPs (Hussein *et al*., 2021). The use of plant extract meets the perspective of green chemistry. Green chemistry perspective has emphasized three main steps for the synthesis of AuNPs: selection of solvent medium

for the synthesis, selection of environmentally friendly reducing agent and the selection of non-toxic material for stabilization of the metal nanoparticles (Pathania *et al*., 2021). Furthermore, plant-based biological synthesis of AuNPs is gaining importance due to its low cost, eco-friendliness, high reproducibility and elaborate process of purification (Pathania *et al*., 2021). Hussein *et al*., (2021) reported the synthesis of mono-disperse punicalagin-stabilized AuNPs by mixing gold solution with an extract of *punica granatum* (pomegranate) fruit peel.

2.5 Nanocomposite

Nanocomposite is a multi-phase solid material where one of the phases has one, two or three dimensions less than 100 nm. The nanocomposite material is a novel product having nano fillers dispersed in the matrix (Kumari *et al*., 2019). The structure of a nanocomposite is a matrix- filler combination where the fillers like particles, fibers or fragments surrounds and binds together as discrete units in the matrix (Kumari *et al*., 2019). However, the preparation method of nanocomposites is challenging due to the control of elemental composition and stoichiometry in the nanophase. As such, the development of an efficient method to produce multi-functional nanocomposites with an appropriate structure is highly required in nanotechnology in order to investigate the full potential of their structural properties and composition of the synthesized products (Argenta *et al*., 2019). Also, production of nanocomposites is vital to be able to examine and evaluate their possible technological usage in various field of study.

Nevertheless, nanocomposites have attracted many researchers and industry because of their potential multi-functional properties from both the nanomaterials and the host materials matrix (Aldosari, 2022). Their unique properties are not depicted by any of the constituent

materials. Typically, the constituent that is present in greater amount is known as the matrix, while the material that is embedded into the matrix in order to improve the mechanical properties of the composites is called reinforcement (or nanomaterials). In general, nanocomposites possess anisotropy properties (properties are directionally dependent) which indicates the distinct property of constituents and inhomogeneous distribution of the reinforcement (Li and Cheng, 2020). These properties touted many researchers to develop interest in nanocomposite material because of its expectation of intense improvements in properties in such areas like life sciences, drug delivery, fuel cell reactors, and energy storage and wastewater remediation. Nanocomposites are classified based on the types of reinforcement materials (nanomaterials) and the matrix material used in their modification (Li and Cheng, 2020).

2.6.1 Synthesis/modification of gold nanocomposite

Different metal and metal oxide nanoparticles with desirable physicochemical properties have been combined with natural and/or synthetic substance to obtain metal nanocomposites. The metal nanoparticles may be composed of gold (Au), silver (Ag), platinum (Pt), and cobalt (Co), nickel (Ni), or copper (Cu), and metal oxide nanoparticles include iron oxide (Fe_3O_4, Fe_2O_3), titanium oxide (TiO_2), zinc oxide (ZnO), or cupric oxide (CuO) as well as metal alloys and salts (De *et al*., 2023). These composites can be made up of metal or alloy matrix filled with nanoparticles, and display physicochemical and mechanical properties that is totally different from those of matrix and/or constituent material (Malaki *et al*., 2019). Metal elemental oxide nanoparticles present antibacterial activity, appropriate optical properties, and electric conductivity, which provide additional properties to its composite. The nanoparticles are generally implanted to improve wear resistance, mechanical properties as

well as damping characteristics and give superior properties to the newly produced composite material (Malaki *et al*., 2019). In addition to this, nanoparticles act as a barrier in dislocation movement and thus improve in the mechanical properties. The covalent bonds that exist between the nanoparticle and the matrix provide strong interactions between them, causing significant changes in the mechanical properties and swelling behaviors of the composite (Argenta *et al*., 2019).

2.6.2 Physicochemical characterization of gold nanocomposite

A variety of analytical techniques have been used to evaluate the physical and chemical of Gold nanocomposite (AuNCs) and they include microscopic, spectroscopic, and calorimetric techniques and X-ray diffraction and are reviewed as follows.

2.6.2.1 *UV-visible spectroscopy*

UV-Visible spectroscopy can be used to obtain the size, aggregation state, and population of nanoparticles of a particular size. The position of plasmonic peak in the UV-Vis spectrum depends on average particle size, whereas its full width at half-maximum depends on the extent of polydispersity of nanoparticles (Pashkov *et al*., 2021). The Principle of UV-Visible Spectroscopy is based on the absorption of ultraviolet light or visible light by chemical compounds, which results in the production of distinct spectra. Spectroscopy is based on the interaction between light and matter. A spectrum is created when the substance absorbs the light through excitation and de-excitation processes. The electrons existing in matter experience excitation when it absorbs UV energy. As a result, they move abruptly from their ground state an energy condition with a negligible amount of energy to their excited state (an energy state with a relatively large amount of energy associated with it). It is significant to remember that the amount of ultraviolet or visible radiation absorbed by an electron is always equal to the energy difference between its ground state and excited state.

Gold nanoparticle exhibit a unique optical feature commonly known as localized surface Plasmon resonance (LSPR), which is the collective oscillation of electrons in the conduction band of gold nanoparticles in resonance with a specific wavelength of incident light. LSPR result in strong absorbance band in visible region (500nm – 600nm) which can be measured by UV-Visible spectroscopy (Yafout *et al*., 2021).

2.6.2.2 *High resolution transmission electron microscopy*

The transmission electron microscope (TEM) operates on the same basic principles as the light microscope but uses electrons instead of light (Emam-Ismail *et al*., 2019). TEM use electron as "light source" and their much lower wavelength make it possible to get a resolution a thousand times better than that with a light microscope with the help of TEM, object can be seen in the order of a few angstroms (10^{-10} m). It can be used to obtain quantitative measures of particle and/or grain size, size distribution, and morphology (Baier and Carmignato, 2022). The magnification of TEM is mainly determined by the ratio of the distance between the objective lens and the specimen and the distance between objective lens and its image plane (Jakubowicz *et* al., 2021). TEM has two advantages over SEM: it can provide better spatial resolution and the capability for additional analytical measurements (Baier and Carmignato, 2022). The disadvantages include a required high vacuum, thin sample section (Jakubowicz *et al.,* 2021) and the vital aspect of TEM is that sample preparation is time consuming. Therefore, sample preparation is extremely important in order to obtain the highest-quality images possible.

High resolution transmission electron microscopy is an imaging mode of the transmission electron microscope that allows the imaging of the crystallographic structure of a sample at

an atomic scale. HRTEM has been widely and effectively used for analysis crystal structures and lattice imperfections to study nanoscale properties of crystalline material such as semiconductors and metals (Baier and Carmignato, 2022).

2.6.2.3 *Energy Dispersive X-ray spectroscopy*

Energy dispersive spectroscopy is a technique used to study the elemental composition in a reaction mixture (Gomathi *et al*., 2020). EDS system are typically integrated into scanning electron microscopy. Shittu *et al*., (2017) reported EDS spectrum reveals strong signals in the silver region and confirm the formation of AuNPs. It was shown that gold (Au 55.08%) was the major constituent element compared to other elements (oxygen, carbon and copper). The energy dispersive spectroscopy (EDS) data showed very strong peaks of gold and weak signals of oxygen, copper and carbon peaks, which indicate the reduction of gold ions to elemental gold possibly originated from the molecules attached to the surface of the AuNPs. EDS also help to determine the percentage purity of the synthesized nanomaterial and also reveals peaks of any impurities present.

2.7 Nano based drug delivery systems

Currently, there has been great development in the area of delivery system to provide therapeutic agents or natural based active compounds to its target location for treatment of several ailments (Obeid *et al*, 2020). There are a number of drug delivery system that have been successfully employed, however, there are still some hiccups that need to be addressed and an advance technology need to be developed for excellent delivery of active agents to their target sites. Hence, nano based drug delivery systems are currently investigated for advanced system of drug delivery. Nano drug delivery systems have been applied in areas significant to skin regeneration, which has evidently accelerate wound healing and improve

healing quality due to several advantages: non-toxicity, perfectly compatible with the skin and favorably create a beneficial moist environment for activation and acceleration of wound healing process (Wang *et al*., 2019). Some nano drug delivery systems are equipped with ability of entering into the cytoplasmic region across cellular barriers or activating specific transport mechanism to improve drug retention (Wang *et al*., 2019). When nano drug delivery systems are incorporated by bioactive agents, the bioactive agents are protected from degradation produced from proteases in wounds, thereby enhancing therapeutic effectiveness (Wang *et al*., 2019).

Nano medicines used for drug delivery are made up of nano scale particles or molecules which can improve drug bioavailability. For maximizing bioavailability both at specific places in the body and over a period of time, molecular targeting is done by nano engineered devices such as nano robots (Niveditha, 2019). The molecules are targeted and delivering of drugs is done with cell precision. In vivo imaging is another area where nano tools and devices are being developed for in vivo imaging. The nano engineered materials are being developed for effectively treating illnesses and diseases such as cancer. With the advancement of nanotechnology, self-assembled biocompatible nano devices can be created which will detect the cancerous cells and automatically evaluate the disease, will cure and prepare reports. The pharmacological and therapeutic properties of drugs can be improved by proper designing of drug delivery systems, by use of lipid and polymer based nano particles (Duan *et* al., 2020). The strength of drug delivery systems is their ability to alter the pharmacokinetics and biodistribution of the drug. Nano particles are designed to avoid the body's defense mechanisms can be used to improve drug delivery (Duan *et al.*, 2020). New, complex drug delivery mechanisms are being developed, which can get drugs through cell

membranes and into cell cytoplasm, thereby increasing efficiency. Tissue damage by drug can be prevented with drug delivery, by regulated drug release. With drug delivery systems larger clearance of drug from body can be reduced by altering the pharmacokinetics of the drug. Potential nano drugs will work by very specific and well understood mechanisms; one of the major impacts of nanotechnology and nanoscience will be in leading development of completely new drugs with more useful behavior and less side effects. Nano drug delivery system also has the ability to sustain drug release and prolong the maintenance of active agent concentration, thereby reducing the frequency of administration (Wang *et al*., 2019). There are two ways through which nano-drug delivery system delivers drug: passive and self-delivery. In Passive delivery, the drug is incorporated in the inner cavity of the carrier mainly through hydrophobic effect. When the nanomaterials are targeted to a particle sites, the intended amount of the drug is released because of the low content of the drugs which encapsulated in hydrophobic environment (Wang *et al*., 2019). Conversely, in self-delivery method, the drugs intended to release are directly conjugated to the carrier nanostructure material for easy delivery. In this method, the timing of release is vital as the drug will not reach the target site and it dissociates from the carrier very quickly and thereby decreasing its bioactivity and efficacy will be decreased if it is released from its nano-carrier at the right time (Wang *et al*., 2019). Targeting of the drugs is another important aspect to take into cognizance and are classified into active and passive. In active targeting, moieties, such as antibodies and peptides are coupled with drug delivery system to anchor them to the receptor structures are regarded as the target site. In passive targeting, the drug carrier complex circulates through the bloodstream and is driven to the target site by attraction or binding influenced by pH, temperature, molecular site and shape. The main targets in the body are

the receptors on cell membranes, lipid components of the cell membrane and antigens or proteins on the cell surfaces (Lei *et al*., 2022).

2.7.1 Inorganic nanoparticle

Inorganic nanoparticles refer to nanoparticles deprived from inorganic materials, such as the metallic nanoparticles, carbon based nanoparticles, ceramic nanoparticles and so on (Khan and Hossain, 2022). Inorganic nanoparticles include silver, gold, iron oxide and silica nanoparticles are included. They showed several advantages such as good biocompatibility and versatility when it comes to surface functionalization. Drugs can be conjugated to gold nanoparticles (AuNPs) surfaces via ionic or covalent bonding and physical absorption and they can be delivered and control their release through biological stimuli or light activation (Amina and Guo, 2020). Silver nanoparticles exhibited antimicrobial activity, but as for drug delivery, very few studies have been carried out,

Banerjee and Qamar (2022), synthesized an inter-linked and spongy polyacrylamide/dextran nano-hydrogels hybrid system with covalently attached silver nanoparticles for the release of ornidazole which turned out to have an in vitro release of 98.5%.

2.8 Application of Nanocomposite in Wound Treatment

Several acute and chronic wounds like burns, mechanical trauma, pressure and leg ulcers, congenital skin diseases and cancer pose a great challenge to the surgeons. Especially burns and skin ulcer are problematic issues (Haidari *et al*., 2023). In most of these cases, the final treatment is autografting, debridement, or use of topical drugs or combination of any aforementioned methods. These methods have been proven to be effective for the treatment of severe wounding conditions due to their biocompatibility features, well-documented

structural, physical, chemical and immunological properties of collage (Haidari *et al*., 2023). These methods have been used successfully in clinic (Haidari *et al*., 2023). Conversely, these wound treatment methods have concomitant flaws thereby creating an unending search for a better and excellent wound treatment methods. Nanomaterials are novel materials that are used for target or specific site delivery of therapeutic agents (Shi *et al*., 2020). Over the years variety of delivery means were designed based on different nanomaterial such as polymers, liposomes, dendrimers, nanorods and nanotubes. However gold nanoparticles have been identified as the best candidate for drug delivery into their specific target site (Gulati *et al*., 2021). The acceptance of AuNPs as an excellent choice for drug delivery was due to its unique properties especially in transportation and release of the therapeutic agents to the target site and non-toxicity to humans (Gulati *et al*., 2021). It has also been reported that AuNPs has unique chemical and physical properties for transporting and unloading the pharmaceuticals. The first pros of AuNPs as a drug carrier is that the gold core is essentially inert and non-toxic, as well as enhanced mechanical stability, resistance against enzymatic degradation when incorporated with active agents (Shi *et al*., 2020), easy incorporation of antibodies, growth factors and peptides at the surface of AuNPs, enhanced biocompatibility, anti-inflammatory and antimicrobial properties (Shi *et al*., 2020). The therapeutic agents to be delivered could be a small a drug, or large biomolecules like proteins, RNA or DNA and effectiveness of their release to the target site is very essential for efficient therapy. There are different factors the influence the release of therapeutic agents to their target sites, internal (glutathione (GSH) or pH, or external light stimuli (Sabourian *et al*., 2020). The internal stimuli control the biological medium while the external stimuli provide spatial control over the release (Sabourian *et al*., 2020). Drugs can be conjugated to gold nanoparticles (AuNPs) surfaces via ionic or covalent bonding and physical absorption and they can deliver them and

control their release through biological stimuli or light activation (Amina and Guo, 2020). Talib *et al*., (2021) penned on using Chitosan-Chondroitin based artemether loaded nanoparticles for Transdermal drug delivery. Gold nanocomposite is defined as a multi-phase solid material where one of the phases has one, two or three dimensions less than 100 nm (Khan and Hossain, 2022). Goldiodine/honey nanocomposite maybe produced by incorporating iodine into AuNPs, using honey to bind the constituent together. Iodine is proven to be effective against all strains of bacteria that inhibit wound healing process. Binding iodine with AuNPs will reduce it toxicity such as skin irritation, dermatitis, scar formation and excruciating pain to human and allow periodic release of iodine into the target area instead of high concentration of iodine to be released in a single application, the iodine is slowly release from the composite over a sustained period of time (Davane *et al*., 2019). Natural honey is used to stabilize the nanocomposite in order to prevent agglomeration thereby keeping the composite complete dispersed. Conversely, honey enables wound healing and prevent the formation of scar after wound healing. However, it has limitation of slow release rate, thereby increasing wound healing period. Thus, conjugating honey and iodine to gold nanoparticle will accelerate the release of both honey and iodine to the wound area and reducing the period of time required for wound to heal. Thus, compositing AuNPs with povidone iodine and pure natural honey will not only curb the individual limitation of the constituent but as well as enhance swift release of the iodine and honey on a wound-bed thereby increasing the therapeutic efficacy of the active agents against certain strains of bacteria (*Staphylococcus aureus, Pseudomonas aeruginosa* and *Escherichia coli*) that cause deleterious effect on an open wound.

2.8.1 Transdermal drug delivery

Excursions of drug concentration in the blood, particularly when the active agent is rapidly absorbed and rapidly eliminated, may lead to periods of underexposure or overexposure. When an active agent is administered from rapid-release dosage forms, a little time is spent inside the so-called therapeutic range. Therefore, frequent repetitive dosing is necessary, with the aim of the maintenance of the effective drug concentration, and compliance and control are difficult. Drug delivery technology has made possible the equalized administration and elimination of an active, resulting in a uniformity of drug concentration in plasma or tissue over the predetermined period of time.

Transdermal patch is a medicated adhesive patch that is placed on the skin to deliver active agent or drug through the skin in order to achieve a systematic absorption of the drug at a predetermined rate over a prolonged period of time. Transdermal patch (skin patch) uses a special membrane to control the rate at which the liquid drug contained in the reservoir within the patch can pass through the skin and into the bloodstream (Alam *et al*., 2021). Some drugs must be combined with substances such as hydrogel, nanocomposite that increases their ability to penetrate the skin in order to be used in a skin patch (Chander *et al*., 2022). Large molecules and many other substances, however are too large to pass through the skin.

Patches applied to the skin eliminate the need for vascular access by syringe or the use of pumps. The major advantages provided by transdermal drug delivery include the following; improved bioavailability, more uniform plasma levels, longer duration of action resulting in a reduction in dosing frequency, reduced side effects and improved therapy due to the maintenance of plasma level up to the end of the dosing interval compared to a decline in plasma levels with conventional oral dosage forms (Wang *et al*., 2019). Transdermal drug

delivery are categories into two; Reservoir type transdermal drug delivery system and Matrix type transdermal drug delivery system. If a drug permeates through the skin at a faster rate than a membrane control system can be made to slow down the penetration rate. Alternatively, if a drug passes the skin at a slower rate than a matrix system incorporating a penetration enhancer should be designed (Chander *et al*., 2022).

In the reservoir system the drug lies between rate-controlling membrane and a backing laminate. The rate of drug release from the reservoir is controlled by the polymeric membrane which may be porous or non-porous (Chander *et al*., 2022).

While in matrix system when a hydrophobic or hydrophilic polymers and active ingredient is homogeneously dispersed then it is known as matrix system (Mehta *et al*., 2021). The amount of drug released depends on the amount of drug held on the matrix and the area of the patch applied to the skin (Mehta *et al*., 2021). Diffusion takes place when the drug passes from the polymer matrix into the external environment (Chander *et al*., 2022).

Table.2.1: Drug Delivery using Gold nanoparticle for Open wound Treatment.

Author (s)	Title	Knowledge gap
Akturk *et al.,* (2016)	Collagen/gold nanoparticle	n a

	nocomposite: A potential wound healing biomaterial The limitation of this research showed that green synthesis method was not employed; neither did it	
Shittu *et al*., (2017)	Application of gold nanoparticle for improved drug delivery efficiency.	Green synthesis of the gold/silver nanoparticles was not employed. The study did not use gold-iodine nanocomposite which is economically friendly than
evaluate the efficiency of collagen/gold nanocomposite against bacteria in wounds. The rate of release of the composite was not also studied using kinetic models. The limitation of this study revealed that gram-negative bacteria was not considered neither did it apply kinetic models to determine the release rate of the drug from the nanoparticle.		
Li *et al*., (2017)	Silver inlaid gold nanoparticle/chitosan wound dressing enhances antibacterial activities and porosity and promotes wound healing.	

Awad *et al*., (2018)	Method of treating diabetic wound using biosynthesized silver/gold nanoparticles Au-Ag-CS. However, the kinetic of release rate of chitosan(CS) was not evaluated.	The study did not use goldiodine nanocomposite which is economically friendly than Au-Ag nanoparicle. Also, the kinetic of release rate was not evaluated; neither were any bacteria preventing wound healing considered.

2.9 Review Summary of Identified Knowledge Gaps

In this thesis, the compositing of gold nanoparticles with active agent agents such as iodine and honey were reviewed. Thereafter, gold nanoparticles were used as delivery vehicle to help transport the active agents (iodine and honey which mediate would healing process) on the strains of bacteria that thwart wound healing. Furthermore, different release kinetic models as postulated in literature was reviewed on the delivery process to determine the best fit.

Little or no research on information has been carried out on drug delivery prowess of gold nanoparticle for open wound treatment. Although, a lot of composite materials have been investigated on bacteria that prevent wound healing. However this research is aiming to close that gap and provide information on the delivery of antibacterial agent (iodine and honey)

using gold nanoparticles on certain strains of bacteria (*Staphylococcus aureus, Pseudomonas aeruginosa, Escherichia coli*) the cause's deleterious effect on open wound healing.

In the course of this work, the green synthesized gold nanoparticle was functionalized with iodine and natural honey. The delivery activity of the gold nanoparticles were investigated in certain strains of bacteria. The detailed experimental protocol and analytical technique used in achieving the aim and various outlined objectives of the research are provided in the next chapter.

2.10 Kinetic of Drug Release

To understand in-vitro drug release, several mathematical models has been postulated to evaluate drug release kinetics such models include zero order model, first order model, Higuchi model, Kosmeyer-peppas model and so on. These models help to estimate the rate of dissolution and diffusion of the drug as well the concentration dependency of the drug released. Several mathematical equations which generally define the dissolution and diffusion profile (El-Hamshary *et al*., 2019). Once an appropriate function has been selected, the evaluation of dissolution profile can be carried out and hence the drug release profile can be correlated with drug release kinetic models.

2.10.1 Zero order model

Considering that dissolution is a kinetic process, the velocity of dissolution reflects the amount of drug dissolved during the time. The dissolution of active agents contained in non-disintegrating dosage forms, considering a very slow drug release (with no changes in the equilibrium conditions), can be represented by equation (2.1);

$$C_t = C_0 + K_0 t \qquad (2.1)$$

C_t is the amount of drug released at time t, C_0 is the initial concentration of drug at time t = 0,

K_0 is the zero-order rate constant. C_t is the amount of drug released at time t, C_0 is the initial concentration of drug at time t= 0,

K_0 is the zero-order rate constant. Hence to study the drug release, kinetics data obtained from *in-vitro* dissolution study is plotted against time i.e., cumulative drug release *vs.* time. Hence the slope of the above plot gives the zero-order rate constant and the correlation coefficient of the above plot will give the information whether the drug release follows zero order kinetics or not. The graphical representation of Equation (2.1) results in a straight, in which the angular coefficient corresponds to K, this relationship can be found in various drug delivery systems (e.g., transdermal slow release matrix, coated, and osmotic systems). For zero-order kinetics, the release of an active agent is only a function of time and the process takes place at a constant rate independent of active agent concentration.

2.10.2 First order

The first order model defines the process of drug release as one whose rate is directly proportional to the concentration of drug undergoing reaction i.e greater the concentration the faster the reaction. Hence it follows a linear kinetic (Patel *et al.*, 2022) which is represented using equation (2.2).

$$\log C_0 - \log C = K_1 t / 2.303 \qquad (2.2)$$

K_1 is the first order rate equation expressed in time (hour), C_0 is the initial concentration of the drug, C is the percent of drug remaining at time t.

Hence to study the drug release kinetics data obtained from *in-vitro* dissolution study is plotted against time i.e., log % of drug remaining *vs.* time and the slope of the plot gives the first order rate constant (Patel *et al*., 2022). Equation (2.2) corresponds to a linear function, and the graph of Napierian or decimal logarithm of the mass released of the drug will result in a straight, with angular coefficient K_1 /2.303 and linear coefficient equal to logC_0.

2.10.3 Higuchi model

The Higuchi model is considered as one of the most widely used well-known controlled release equation which envisages the study of release of drug from a drug delivery system involve both dissolution and diffusion (Ailincai and Marin, 2020). 'Higuchi equation' as represented in equation (2.3) has become a prominent kinetic equation in its own right, as evidenced by employing drug dissolution studies that are recognized as an important element in drug delivery development (Ailincai and Marin, 2020). The model explained the released of drugs from and insoluble matrix as square root of time dependent process based on Fickan diffusion (Das *et al*., 2021).

$$C = K_H t^{1/2} \tag{2.3}$$

Where, K_H is the Higuchi dissolution constant.

The data obtained were plotted as cumulative percentage drug release versus square root of time. Therefore, the simple Higuchi model will result a linear Q versus $t^{1/2}$ plot having gradient, or slope, equal to K_H and we say the matrix follows $t^{1/2}$ kinetics (Das *et al*., 2021). Hence if the correlation coefficient is higher for the above plot then we can interpret that the prime mechanism of drug release is diffusion controlled release mechanism. It is important to note that a few assumptions are made in this Higuchi model. These assumptions are: (i)

the initial drug concentration in the system is much higher than the matrix solubility. (ii) Perfect sink conditions are maintained. (iii) The diffusivity of the drug is constant and (iv) The swelling of the polymer is negligible. The sink conditions are achieved by ensuring the concentration of the released drug in the release medium never reaches more than 10 per cent of its saturation solubility.

2.10.4 Korsmeyer-peppas model

Once it has been ascertained that the prime mechanism of drug release is diffusion controlled from Higuchi plot then it comes the release of drug follows which type of diffusion. To understand the dissolution mechanisms from the matrix, the release data were fitted using the well-known empirical equation proposed by Korsmeyer and Peppas (Patel *et al*., 2022). Korsmeyer and Peppas put forth a simple relationship which described the drug release from a polymeric system follow which type of dissolution and it's represented in equation (2.4).

$$\log(Mt/M\infty) = \log K_{kp} + n\log t \qquad (2.4)$$

Mt is the amount of drug released in time t, M∞ is the amount of drug released after time ∞, n is the diffusion exponent or drug release exponent, K_{kp} is the Korsmeyer release rate constant.

To study release kinetics a graph is plotted between log cumulative % drug release log(Mt/M∞) *vs.* log time (log t) (Das *et al*., 2021).

The power law model is useful for the study of drug release from polymeric systems when the release mechanism is not known or when more than one type of phenomenon of drug release is involved (Patel *et al*., 2022). Actually, it can be seen as a generalization of the observation of the superposition of two apparently independent mechanisms of drug

transport, relaxation, and diffusion. Depending on the value of n that better adjusts to the release profile of an active agent in a matrix system, it is possible to establish a classification, according to the type of observed behavior: Fickian model (Case I) and Non-Fickian models (Case II, Anomalous Case and Super Case II).

In the Fickian model (Case I), $n = 0.5$ and the drug release are governed by diffusion. The solvent transport rate or diffusion is much greater than the process of polymeric or nanoparticle chain relaxation. Equilibrium of absorption in the surface exposed of the polymeric system takes place rapidly, leading to conditions of time-dependent links. The kinetics of this phenomenon are characterized by diffusivity. When $n=1$, the model is nonFickian (Case II), the drug release rate corresponds to zero-order release kinetics and the mechanism driving the drug release is the swelling or relaxation of polymeric chains this is another extreme type of behavior. At the end of Case II transport, a fast increase of absorption rate of solvent may sometimes be observed. In this situation, the transport Case II evolved to transport Super Case II, due to the expansion of forces exercised by swollen gel in the vitreous nucleus. Moreover, when $0.5<n<1$, the model is non-Fickian or anomalous transport, and the mechanism of drug release is governed by diffusion and swelling.

CHAPTER THREE

3.0 MATERIALS AND METHODS

3.1 Materials, Reagents and Equipment

The equipment and apparatus used in this study are listed in Table 3.1, while the list of chemicals/reagents used in this study are listed in Table 3.2 with their percentage purity and suppliers.

Table 3.1: List of Equipment/Apparatus

Equipment	Model	Manufacturer	Location
Magnetic Stirrer	78HW-1	Gallenkamp, UK	FUT, Minna
UV spectrophotometer	Shimadzu uv1800	England	FUT, Minna

	Zeiss Auriga	FEI, Netherland	
High resolution Transmission electron microscope			University of Western Cape, South-Africa
Autoclave	Gallenkamp	Gallenkamp, U.K	
Incubator	Gallenkamp	Gallenkamp, U.K	Jesil Pharmaceutical Limited, Minna FUT Minna

Table 3.2: List of Reagents/Chemicals Used

Name	**Formula**	**% purity**	**Place of manufacture**
Chloroauric acid	$HAuCl_4$	99	Sigma Aldrich, Germany
Povidone Iodine	I_2	10	Nahson science laboratory, Minna
Nutrient Broth	-	NA	Sigma Aldrich, Germany
Centrimiole agar	-	NA	Sigma Aldrich, Germany
Nutrient agar	-	NA	Sigma Aldrich, Germany
Manitol salt agar	-	NA	Sigma Aldrich, Germany
Methylene blue agar	-	NA	Sigma Aldrich, Germany
Hydrochloric acid	HCl	35.5	Merk, Germany
Sodium Hydroxide	NaOH	98	Lobachemie

Key:

NA: Not Available

3.1.2 Collection and Identification of Plant Materials

Fresh *Agerantum conyzoides* plants were collected from a farm in Minna metropolis during dry season and was taken to the Department of Plant Biological, Federal University of Technology, Minna for botanical identification.

The natural honey samples were collected from a local bee-farmer in Suleja, Niger State into a cleaned high-density polythene sampling bottles and subsequently transported to the laboratory for analysis.

Povidone Iodine (10% w/v) was purchased from NAHSON science laboratory within Minna metropolis. Analytical grade gold chloride ($HAuCl_4$) (99.0 %) was purchased from Sigma-Aldrich Chemicals, Germany.

The following bacterial pathogens; *Escherichia coli* (gram negative), *Pseudomonas aeruginosa* (gram negative) and *Staphylococcus aureus* (gram positive) used were isolated from chronic wound patients from the Microbiology Department of General Hospital, Minna. They were sub cultured into Nutrient Agar slants and kept in the refrigerator until they were ready for use.

3.2 Preparation of Crude Plant Extract

The air dried plant parts (leaves) were ground to powder using a blender. The extraction was carried out via aqueous extraction method as described by Shittu *et al*. (2017). The extract was prepared by measuring 5 g of the fine powder into 100 cm^3 sterile distilled water in a beaker and boiled at 60 °C for 1 h. The crude extract was allowed to cool for 30 minutes at room temperature (24±5 °C). This crude extract was filtered twice using Whatman No. 1

filter paper with pore size 0.7 µm in order to obtain a clear filtrate. The filtrate was then stored in an air-tight amber bottle and kept in the refrigerator for further analysis.

3.2.1 Phytochemical screening of the plant crude extract and natural honey The crude extracts and pure honey were subjected to phytochemical analysis to screen for the presence of some secondary metabolites such as alkaloids, reducing sugar, saponins, flavonoids, phenols and tannins. The phytochemical screening was carried out using standard procedure (Hariani *et al*., 2022).

3.2.1.1 ***Test for Alkaloids***

This was carried out according to the method employed by Sadh *et al*., (2018). 0.50 g of the extract was weighed and dissolved in 5 cm^3 of mixture of 96 % ethanol and 20 % tetraoxosulphate (vi) acid (1:1). The entire solution was filtered through Whatman No. 1 filter paper. 1 cm^3 of the filtrate was added to a test tube containing 5 cm^3 of 60 % H_2SO_4 and allow to age for 5 minutes. Thereafter, 5 cm^3 of 0.5 % formaldehyde was added and allowed to stand at room temperature for 3 hours. Vincristine extinction co-efficient (E296, ethanol {ETOH}=15136 $m^{-1}cm^{-1}$) was used as standard alkaloids.

3.2.1.2 ***Test for Flavonoids***

Exact 0.2 g of the extract was diluted with five drops of dilute NaOH. The appearance of a yellow solution which disappeared on addition of few drops of dilute hydrochloric acid indicated the presence of flavonoids.

3.2.1.3 ***Test for Saponins***

An aliquot of 5 g of the crude extract was shaken vigorously for 2 minutes with 10 cm^3 of distilled water in a test-tube. Frothing or persistent foaming revealed the presence of saponins.

3.2.1.4 *Test for Tannins*

The method of Association of Official Analytical Chemist (AOAC, 2002) adopted by Muthuraj (2019) was employed for the determination of tannins content in the plant extracts. 0.2 g of the extracts were weighed into a 100 cm^3 beaker and 20 cm^3 of 50 % methanol was added to it and covered with foil paper and heated in water bath shaker at 80 °C for 1 hour. This was then filtered into a 100 cm^3 volumetric flask and 20 cm^3 of distilled water, 2.5 cm^3 of Follin-Denis reagent, and 10 cm^3 of Na_2CO_3 (0.5 $moldm^{-3}$) were added and shaken vigorously. The reaction mixtures were allowed to stay for 20 minutes at room temperature for the formation of bluish-green coloration. Standard tannic acid was used to prepare the calibration curve. The absorbance was measured at 760 nm.

3.2.1.5 *Test for Phenols*

One gram (1 g) of crude extract and $FeCl_3$ was mixed and vortexed for 2 minutes. The formation of violet colouration revealed the presence of phenols.

3.2.1.6 *Test for reducing sugars (Fehling's test)*

Zero point two grams (0.2g) of extract was dissolved in water and filtered into a test tube. The filtrate was then heated with 5 cm^3 of Fehlings A and B solution each. The formation of red precipitate of cuprous oxide indicated the presence of reducing sugars.

3.2.2 Green synthesis of gold nanoparticles (AuNPs)

Exact 5 cm^3 of *Agerantum Conyzoides* leave extract was added to 25 cm^3 of 1$moldm^{-3}$ of aqueous solution $HAuCl_4$ at a ratio 1:5 (v/v). The resulting mixture was stirred at 180 rpm at room temperature under static condition for 15 minutes. The formation of gold nanoparticles were confirmed by a colour change of the reaction mixture (yellow to dark ruby).

Confirmation of colloidal gold nanoparticles formation by the reduction of Au^{3+} from $HAuCl_4$ to Au^0 was monitored using UV-Visible spectrophotometer.

3.2.3 Formulation of Gold Nanoparticle (AuNPs) into Au-INCs, Au-HoneyNCs and Au-I/HoneyNCs.

The modification/functionalization of the gold nanoparticles (AuNPs) was carried out using 10 % Iodine solution and honey. The loading of gold nanoparticles with povidone iodine was achieved by the addition of 50 cm^3 of the green synthesised AuNPs with 10 cm^3 of iodine solution. The solution was kept under stirring a hot plate with magnetic stirrer at 180 rpm for 30 minutes at 60 °C, and later ultrasonicated for 45 minutes so as to allow more dispersion and effective doping. Second formulation (composite of AuNPs with natural honey) was obtained by adding 10 cm^3 of honey to 50 cm^3 of AuNPs and stirred on magnetic stirrer at 180 rpm for 1 h. The third formulation (composite of Au-INCs with honey) was prepared by mixing 10 cm^3 of honey with 50 cm^3 of Au-INCs and stirred on magnetic stirrer for 1 hour at 180 rpm, and later ultrasonicated for 30 minutes so as to allow more effective doping. All the formulations were made into semi-solid by freeze drying.

3.2.4 Characterisation of AuNPs, Au-INCs, Au-HoneyNCs and Au-I/Honey-NCs

Gold nanoparticles, gold-honey nanocomposite and gold-iodine nanocomposite stabilized on natural honey were characterized using UV-visible spectrophotometer, HRTEM and EDS.

3.2.4.1 *UV-Visible Spectroscopy of Green Synthesized AuNPs*

The lambda maximum (λ_{max}) of the green synthesized nanoparticles were analysed using a UV-Visible Spectrophotometer in the wavelength range of 200-800 nm using quartz cuvettes. A known volume (3 cm^3) of each of the prepared nanoparticles was poured into a quartz cuvette. The cuvette containing the sample was placed into the cuvette holder for

measurement. Prior to sample measurements, background measurement was carried out using two empty pre-cleaned quartz cuvettes to subtract the interferences.

3.2.4.2 *High Resolution Transmission Electron Microscope (HRTEM) of Green Synthesized AuNPs, Au/INCs and Au/I-HoneyNCs*

To characterise the size, shape and microstructure, HRTEM coupled with SAED were utilised. 20 mg of the samples were dispersed in 10 cm^3 of methanol and the mixture was ultrasonicated for 40 minutes. Two drops of the nanoparticles suspension or slurry were dropped onto the carbon coated copper grid (400 mesh) with the aid of micropipette and dried at room temperature. After drying, the grid was loaded on the single-tilt sample holder and subsequently mounted onto the shaft of the electron microscope, and the internal structure of the image was determined (Sermakkani and Thangapandian, 2012).

3.2.5 Confirmatory test for the bacteria pathogen

The selected bacteria were all confirmed using streaking method in their respective agar prior to use.

3.2.5.1 ***Confirmation of Escherichia coli using Eosin Methylene Blue Agar (EMB)*** Three point six grams (3.6 g) of eosin methylene blue agar was dissolved in 100 cm^3 of distilled water; the medium was autoclave for purification at 121°C for 15 minutes. The solution was distributed into a sterile petri plate, allowed to cool and solidify. Sterile inoculating loop was used to pick up some culture of bacteria colony from the agar slant to streak on the first quadrant of the EMB agar plate. The inoculating loop was sterilized again
(burn and allow to cool) and used to streak on the second, third and fourth quadrant of the

EMB plate to complete the streaking. The inoculated EMB plate was incubated at 37 °C for 24 h. After incubation, the colonies grown were observed on the plate. Metallic green sheen on the plate confirmed the presence of *Escherichia coli* (Cheesbrough, 2005).

3.2.5.2 *Confirmation of Pseudomonas Aeruginosa using Centrimiole Agar*

Five grams (5.0 g) of centrimiole agar was dissolved in 100 cm^3 of distilled water; the medium was autoclave for purification at 121 °C for 15 minutes. The solution was distributed into a sterile petri plate, allowed to cool and solidify. Sterile inoculating loop was used to pick up some culture of bacteria colony from the agar slant to streak on the first quadrant of the centrimiole agar plate. The inoculating loop was sterilised again (burn and allow to cool) and used to streak on the second, third and fourth quadrant of the centrimiole plate to complete the streaking. The inoculated centrimiole plate was incubated at 37°C for 24 hours. After incubation, the colonies grown were observed on the plate. A green pigment on the plate confirmed the presence of *Pseudomonas aeruginosa* (Cheesbrough, 2005).

3.2.5.3 *Confirmation of Staphylococcus Aureus using Manitol Salt Agar*

Seven grams (7.0 g) of manitol salt agar was dissolved in 100 cm^3 of distilled water; the medium was autoclave for purification at 121°C for 15 minutes. The solution was distributed into a sterile petri plate, allowed to cool and solidify. Sterile inoculating loop was used to pick up some culture of bacteria colony from the agar slant to streak on the first quadrant of the manitol agar plate. The inoculating loop was sterilized again (burn and allow to cool) and used to streak on the second, third and fourth quadrant of the manitol agar plate to complete the streaking. The inoculated manitol plate was incubated at 37°C for 24 hours. After incubation, the colonies grown were observed on the plate. Yellow colonies of

Staphyloccocus aureus on the plate confirmed the presence of *Staphyloccocus aureus* (Cheesbrough, 2005).

3.2.6 Application of gold-iodine nanocomposite stabilized on honey

The *in-vitro* drug release study of gold-iodine nanocomposite and gold-iodine/honey nanocomposite were studied by dialysis bag diffusion method. 25 cm^3 of Gold-iodine nanocomposite containing 0.794 $moldm^{-3}$ of povidone iodine was dispersed in dialysis bag kept in a beaker containing 300 cm^3 of the cultured multi-resistance bacteria (*Escherichia coli* (gram negative), *Pseudomonas aeruginosa* (gram negative) and *Staphylococcus aureus* (gram positive)) to mimic an open wound bed, the population of bacteria introduced into the cultured media was determined using Mcfarland standard. The beaker was placed over a magnetic stirrer and the temperature of the assembly was maintained at a room temperature throughout the experiment. 4 cm^3 of the cultured media were withdrawn at a definite time interval and replaced with fresh equal amount of the cultured bacteria. After suitable dilutions, the samples were analyzed using UV-Visible spectrophotometer at 540 nm, to determine the concentration and absorbance of the cultured bacteria (Oloninefa *et al*., 2018). The experiment was carried out on these strains of bacteria *Staphylococcus aureus, Pseudomonas aeruginosa* and *Escherichia coli*.

3.2.7 Evaluation of the drug-release analysis

To evaluate the *in-vitro* drug release data several kinetics models include zero order model, first order model, Higuchi model and Kosmeyer-peppas model were applied to describe the rate and mechanism of release of the nanocomposite. Once an appropriate function has been selected, the evaluation of dissolution profile carried out and hence the drug release profile

correlated with drug release kinetic models. The mathematical models and their equations are shown in Table 3.3.

Table 3.3: Mathematical models used to study the kinetic of drug release (Bohrey *et al*., 2016)

Mathematical model	**Equation**
Zero order release model	$C_t = C_0 + K_0t$
First order release model	$\log C_0 - \log C = K_1t /2.303$
Higuchi release model	$C = K_Ht_{1/2}$
Kosmeyer-peppas model	$\log(Mt/M\infty) = \log K_{kp} + n\log t$

Key: C_t = amount of drug released at time t; C_0 = initial concentration of drug at time t = 0; K = rate constant; C = amount of drug remaining at time t; t = time (hours); K_H = Higuchi dissolution constant; Mt = amount of drug released in time t; $M\infty$ = amount of drug released after time ∞; n = drug release exponent; K_{kp} is the Korsmeyer release rate constant**.**

CHAPTER FOUR

4.0 RESULTS AND DISCUSSION

4.1 Phytochemical constituents of *Agerantum conyzoides* plant extract and Natural Honey

The qualitative phytochemical screening of *Agerantum conyzoides leaves* extract and pure honey revealed the presence of major secondary metabolite such as phenols, tannins, saponnins and flavonoids. While alkaloids are present in the plant extract but absence in pure honey, the reverse is the case for reducing sugar as shown in Table 4.1. The presence of these (alkaloids, tannins, phenols and saponnis) essential secondary metabolites in the plant extracts helped to mediate the green synthesis of gold nanoparticles (AuNPs) using $HAuCl_4$ as the gold precursor.

Table 4.1: Some phytochemical constituents of *Agerantum conyzoides* plant extract and Natural Honey

Phytochemicals	***Agerantum Conyzoides***	**Natural honey**
Tannins	+	+
Saponins	+	+
Flavonoids	+	+
Phenols	+	+
Reducing Sugar	-	+
Alkaloids	+	-

Key: - Present (+), Absent (-)

Phenols is an aromatic organic compound which consists of hydroxyl groups that can act as reducing agents. Aslam *et al*. (2021) reported the synthesis of gold nanoparticles using an aqueous extract of *Hovenia dulcis* fruit and the authors described that the hydroxyl, carboxyl groups and other bioactive molecules in water extract first bind with the gold ions to form gold complexes, which were reduced to seed particles (Au^0). The reduced seed particles clusters, which act as nucleation centers and catalyze the reduction of remaining metal ions into nanoparticles. Therefore, the presence of this biomolecules at a reasonable concentration in the plant extract enabled it to serve as reducing and capping agent for the gold. Flavonoids are polyphenolic compounds found in plant. It is a powerful antioxidant with reducing capability. Tannins which are water soluble polyphenolic biomolecules have been reported as reducing and stabilizing agents in the synthesis of silver nanoparticles (Shittu *et al.,* 2017). Several studies have reported that these phytoconstituents play a leading role in the

biochemical reduction of gold ions to gold in zero valent state (Ovais *et al*., 2018), as well as stabilizing and capping agents to the nanoparticles.

Furthermore, these phytochemical components present in both plant extracts and pure honey are also responsible for their effectiveness against many microbes and also enable them to function as herbs or drugs by producing biological activity in animals and in humans (Shittu *et al.*, 2017). Flavonoids contain many beneficial pharmacological properties such as anti-inflammatory, antibacterial and have antioxidant potentials which could offer great protection by enhancing the defense of the body against infections caused by the generation of free radicals (Mitra *et al*., 2022). The flavonoids also possess activities such as anti-allergic, antitumor, vascular and cytotoxic activities as stated in the work of

Mitra *et al*. (2022).
Phenols, one of the famous phytochemicals have very wide pharmacological activities. These activities include: antitumor, antispasmodic, antidepressant, antioxidant, cytotoxic, anti-inflammatory and antiulcer (Abdullahi and Hamza, 2020).

The results of this study show that *Agerantum conyzoides* leaves extract and natural honey consist of many bioactive compounds which suggests their potential to be used as an alternative therapeutic agent for a number of medical conditions, particularly bacterial infections on open wound healing.

4.2 Characterization of Green Synthesized Gold nanoparticle (AuNPs) and Modified Gold Nanoparticle with Povidone Iodine and Honey

The characterization results of gold nanoparticles and modified gold nanoparticles using iodine and natural honey are as follows.

4.2.1 UV-Visible spectroscopy of gold nanoparticle and gold-based nanocomposites.

UV–Vis spectroscopy presented in Figure 4.1(a), revealed a single broad plasmon band for pure AuNPs at 548 nm which a peculiar plasmon band of AuNPs (500 – 600 nm). This result obtained did not correlate well with the report stated by Shittu *et al*., (2017) due to disparity in the broad plasmon band of 533 nm. The observed differences may be linked to different plant material (which were grown under different environmental factors) including different reaction time and volume ratio. The observed wavelength and colour change during the reduction of Au^{3+} to Au^{0} is an indication of formation of gold nanoparticles.

On incorporation with honey as shown in Figure 4.1(b), the intensity of the broad peak at 548 nm decreases due to interaction with different functional groups present in honey thereby causing a hypochromic shift (a decrease in absorptivity) in the plasmon band.

Studies have revealed that honey has suppressive and capping effect on nanoparticle (Ghramh *et al*., 2021).

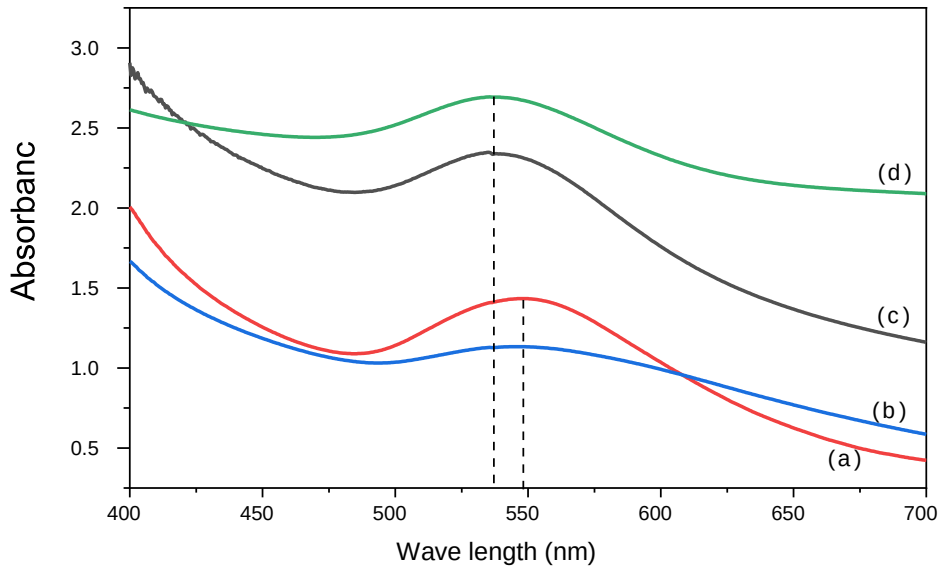

Figure 4.1:- Absorption spectra (a) AuNPs (b) Au-honeyNCs (c) Au-INCs (d) Au-

I/honeyNCs

Figure 4.1(c) reveals UV-visible spectra of modified gold nanoparticles with iodine, it clearly reveals a single plasmon band at 536 nm, which shows increased intensity of the plasmon and an evidence of slight blue shift (to a shorter wavelength) in the plasmon band. This effect may be attributed to the chelation of iodine with gold nanoparticle thereby causing a change in the dielectric constant of the surrounding medium (Ghramh *et al*., 2021). Hence, the presence of iodine may have increased the electronegativity of the gold nanoparticle. Increase in electronegativity decreases the excited wavelength, because when electronegativity increases the electron cloud density slightly shifted towards LUMO (lowest unoccupied molecular orbital) (Ghramh *et al*., 2021). However, on supporting the gold-iodine nanocomposite with honey, the intensity of the plasmon band (536 nm) increases as well as its concentration as shown in Figure 4.1d. This may be due to increase in particle size and interaction of the gold nanoparticle with several functional groups present in honey and iodine. This result is in agreement with the findings of Sun *et al*., 2015 who studied the effect of iodide on gold nanoprism. The unique color (optical properties) which was visually observed in the reaction mixture (Plate III) and the appearance of the absorbance peaks (Figure 4.1a) can be ascribed to surface plasmonic resonance of gold (John *et al*., 2018).

(a) **(b)** **(c)**

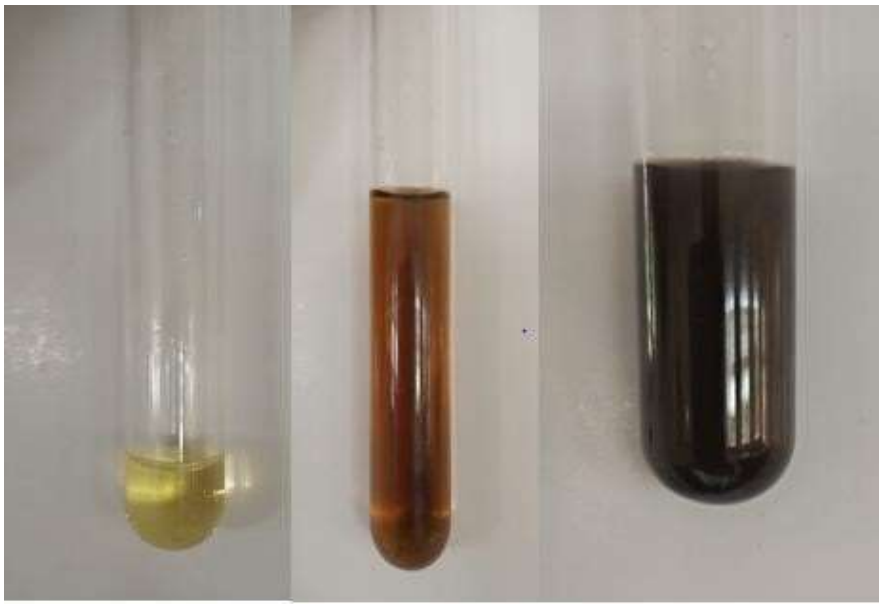

Plate III:- (a) Gold chloride solution (b) Plant extract (c) Colloidal gold nanoparticle

4.2.2 HRTEM images of gold nanoparticle

The high-resolution transmission electron microscopy (HRTEM) monograph of colloidal gold nanoparticle is shown in plate III. Gold nanoparticles are well dispersed and exhibits various size ranges as well as different shapes majorly spherical and quasi-spherical. The spherical morphology of the HRTEM images of the gold nanoparticle may be due to the addition of plant extract as a reducing agent which may cause an effective collision of the particle and prevention of agglomeration of the gold nanoparticle.

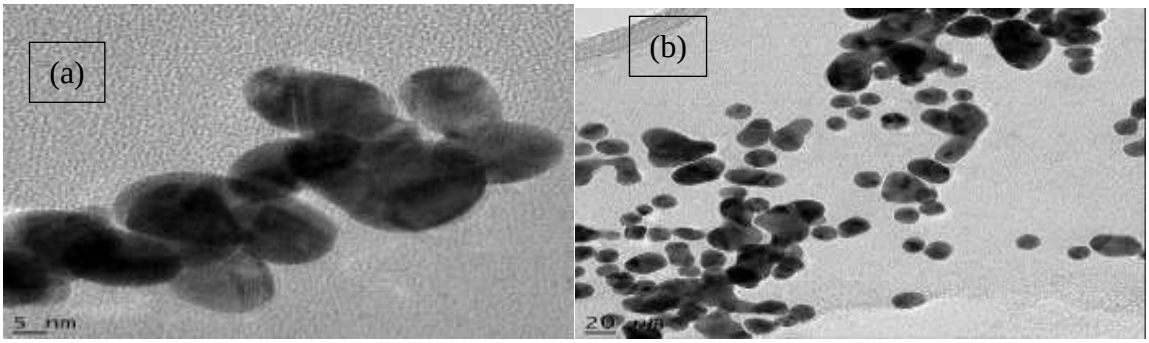

Plate IV: - HRTEM high and low magnification images of gold nanoparticle

The AuNPs particles sizes are in the range of 6 – 24 nm, where the average particle size was estimated to be 13.08 nm as measure by Image J. Figure 4.2a shows the histogram of the particle size distribution of AuNPs. It clearly reveals a wide variation in the particle size distribution of the synthesized AuNPs which is a signature of its polydispersity. Similar trend has also been reported by Shittu *et al*., (2017) who synthesized gold nanoparticle particle using aqueous extract of *Khaya senegalensis* stem.

4.2.3 SAED pattern and EDX analysis of gold nanoparticle

The elemental composition of the biosynthesized gold nanoparticle was determined by Energy Dispersion X-ray analysis (EDX). Area profiling of the biosynthesized nanoparticle in Figure 4.2b showed strong peak of gold confirming the formation of gold nanoparticle. The maximum absorption peak of gold is located at 2.1 keV. It was confirmed that Au peaks were predominant in the area profile which is a signature that the synthesized gold nanoparticles have high purity. The presence of peaks such as carbon and copper was also detected which can be attributed to the nature of grid used for analysis.

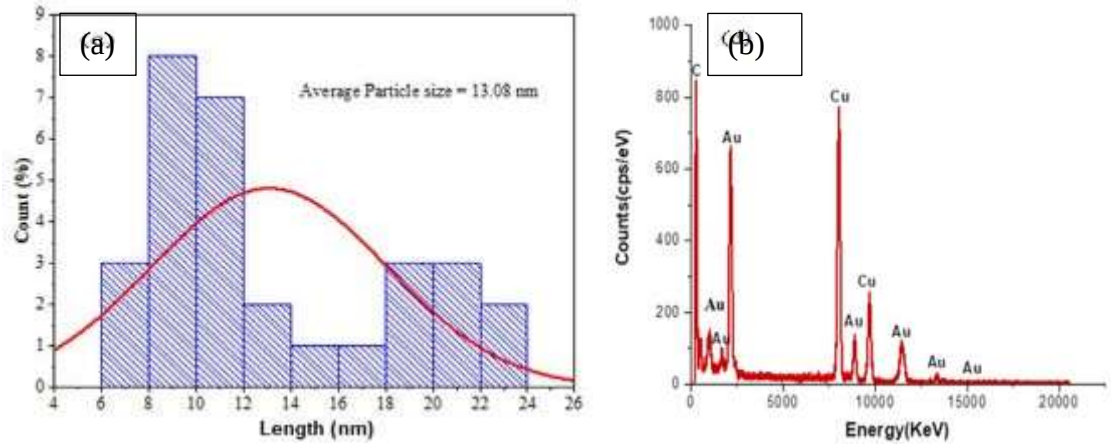

Figure 4.2:- (a) Particle size distribution of gold nanoparticle (b) EDX profile of gold nanoparticles (AuNPs)

The SAED in Plate IV shows separated diffraction rings from inner to outer atomic planes with discrete spots(atoms) indicating the formation of polycrystalline gold nanoparticles. This trend has also been reported by Shittu *et al*., (2017) in the synthesis of gold nanoparticle using aqueous extract of *Khaya senegalensis* stem.

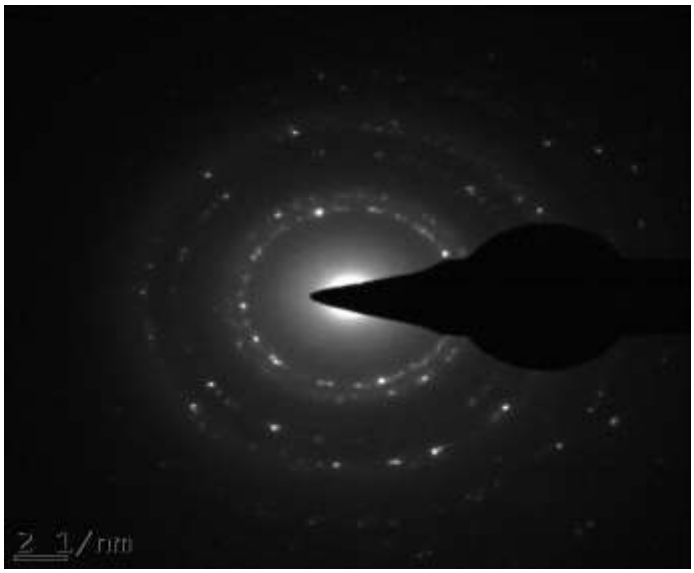

Plate V:- Selected Area of Electron Diffraction (SAED) pattern of AuNPs

4.3 HRTEM Images of the Gold Based Nanocomposites

Plate V (a, b and c) clearly shows the HRTEM high and low magnification images of the gold based nanocomposite. Plate V (a) reveals the aggregation/fusing of spherical shaped AuNPs on the surface of honey. This may be as a result of the capping or binding effect of honey on the AuNPs which may cause an effective collision of the particles and prevention of agglomeration of the AuNPs. The Au-honeyNCs were well dispersed and exhibit various particle sizes distribution with an average particle size of 14.97 nm. The Au-honeyNCs

exhibit polydispersity in sizes. This is consistent with the findings of Manju and Savi, (2018) in the synthesis of gold nanoparticle using natural honey as the reducing agent.

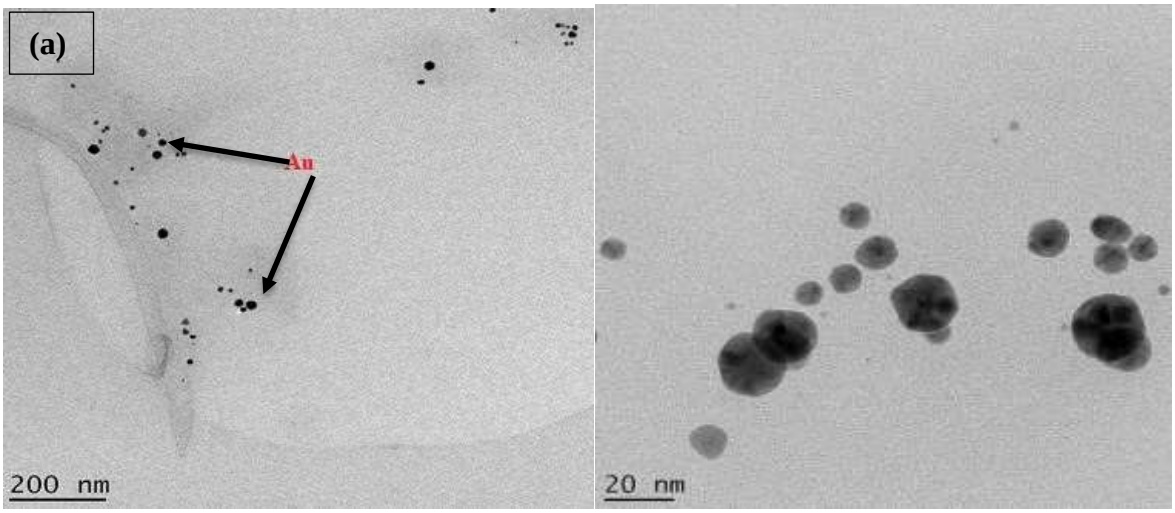

Plate VI (a):- HRTEM high and low magnification images of (a) Au-honeyNCs

Plate VI (b) reveals a sintered mixture of AuNPs and iodine having a roughen surface due to the latter forming a chelating ligand around the former. At higher magnification, the HRTEM image shows that Au-INCs are spherical in shape and exhibits polydispersity in particle sizes with an average particle size of 32.60 nm. It is evidence that the presence of iodine has brought about significant increase in the particle size.

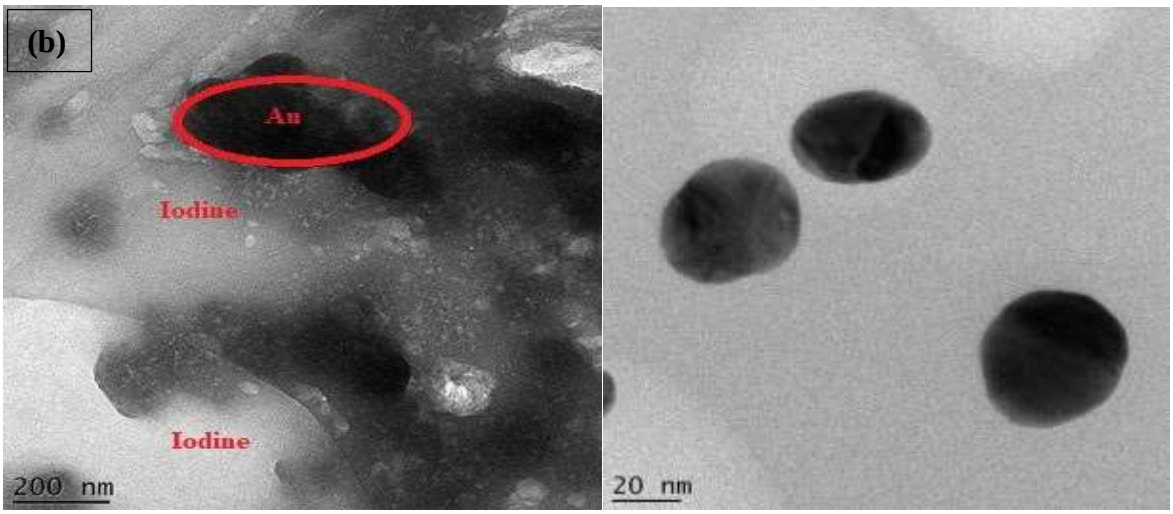

Plate VI (b):- HRTEM high and low magnification images of Au-INCs.

On incorporation of honey into Au-INCs, the HRTEM image in Plate V(c) reveals a distinctive spherical shape Au-I/honeyNCs which are well dispersed and exhibits monodispersity in particle sizes distribution with an average particle size of 37.57 nm. The monodispersity maybe as a result of honey that has capped most of the Au-INCs particle into same size ranges. It is evidence that the presence of honey acts as binder which may have caused an effective collision between AuNPs and Iodine solution thereby preventing the emerging nanocomposite from sintering and with small increase in particle sizes compare to Au-INCs. Similar trend was observed in the findings of Walsh, (2017) on chemisorption of iodine to gold nanoparticle.

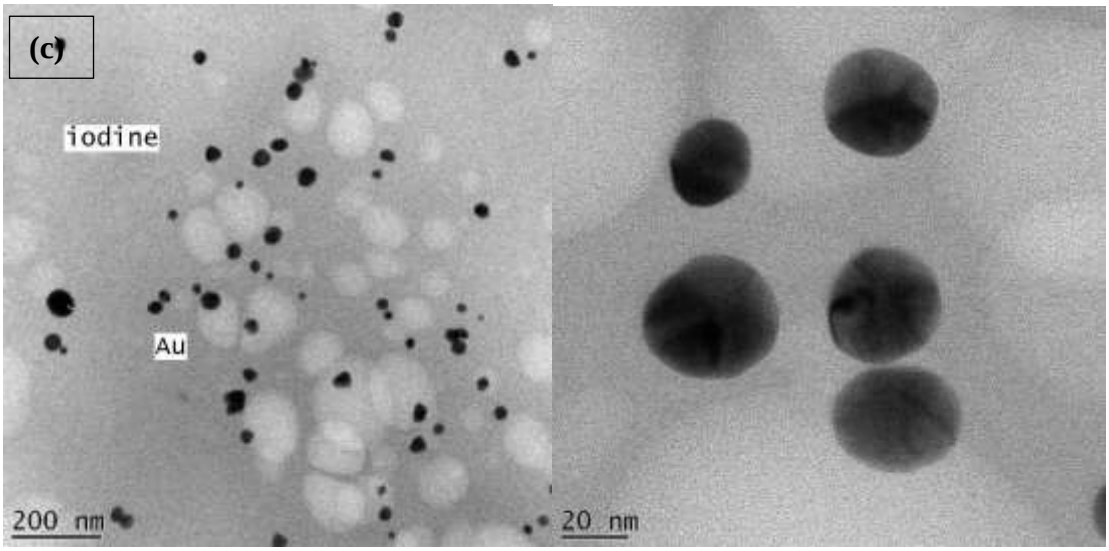

Plate VI (c):- HRTEM high and low magnification images of Au-I/honeyNCs

4.3.1 Particle size distribution of the gold-based nanocomposites

Figure 4.3(a, b & c) shows the particle size distribution of Au-honeyNCs, Au-INCs and Au-I/honeyNCs respectively. In Figure 4.3(a), the size distribution of Au-honeyNCs ranging

from 5.98 nm to 22.98 nm. Wide variation in particle sizes was observed, which is a signature of the polydispersity of Au-honeyNCs.

For Au-INCs as shown in Figure 4.3(b), the particle size distribution ranging from 13.93 to 49 nm with an average particle size of 32.60 nm. The maximum number of Au-INCs was around 40 nm. From the histogram in Figure 4.3b it is observed that there is wide variation in the particle sizes of Au-INCs which is an indication of its polydispersity.

Figure 4.3(c) reveals the particle size distribution of Au-I/honeyNCs ranging from 15.15 to 65 nm. The average particle size was measured to be 37.57 nm where maximum number of Au-INCs was around 40 nm. This close similarity in the particle sizes confirm that Au-I/honeyNCs are monodispersed.

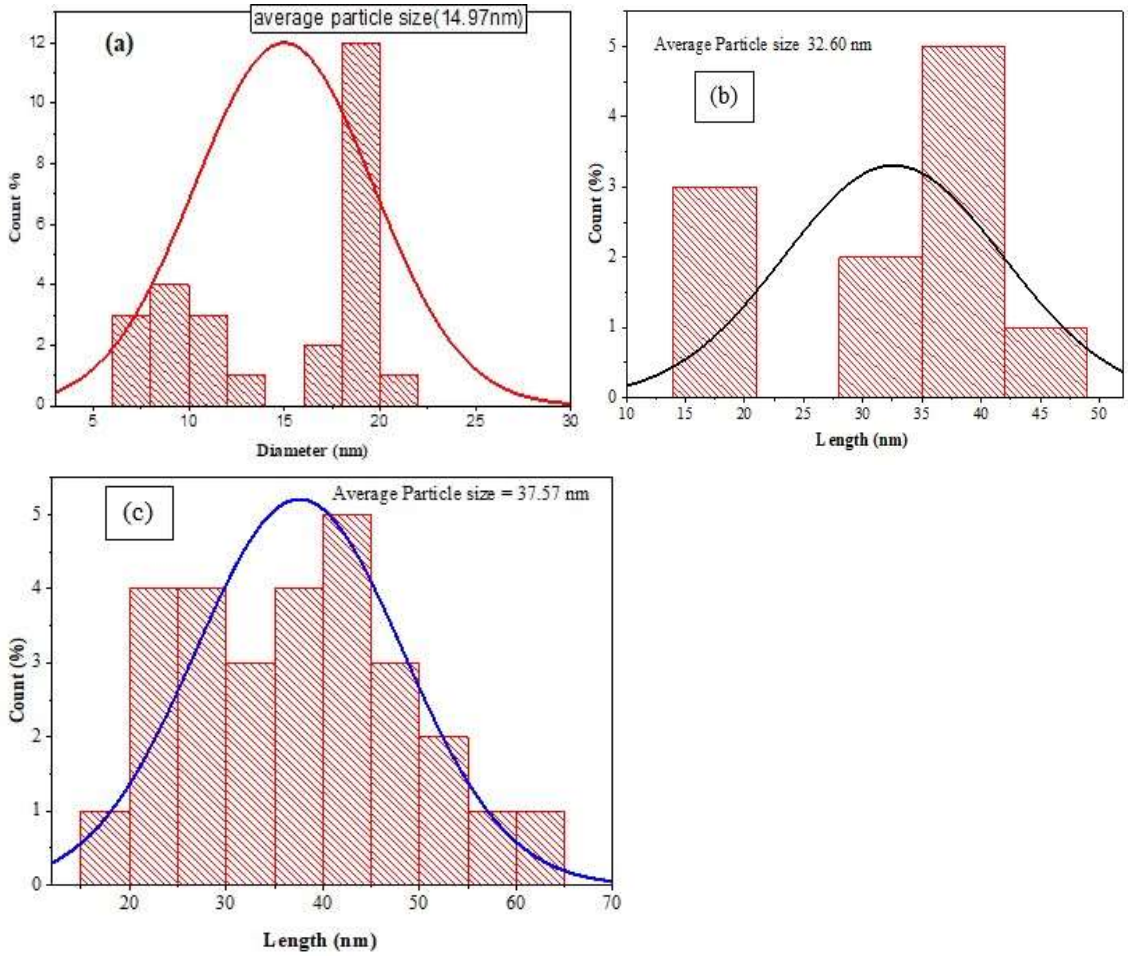

Figure 4.3: Particle size distribution of (a) Au-honeyNCs (b) Au-INCs (c) Au-I/honeyNCs

4.4 Selected Area of Electron Diffraction (SAED) Pattern of Gold based nanocomposites

The elemental composition of the modified Au-honeyNCs, Au-INCs and Au-I/honeyNCs were further studied using selected area electron diffraction. The SAED pattern of AuhoneyNCs as shown in plate VII (a) reveals well-separated concentric rings with few discrete spots (atoms) which is predominant on the first inner ring. This is an indication that AuNPs supported on honey is partly polycrystalline. This also corroborates with the findings of Manju and Savi (2018) who obtained bright concentric rings of gold nanoparticle inlaid on honey matrix.

Plate VII (b) depicts the SAED pattern of Au-INCs showing the presence of diffuse rings with no discrete spots which is signature that gold-iodine nanocomposite is amorphous. The non-crystallinity of gold-iodine nanocomposite is attributed to the complete dissolution of gold nanoparticle in iodine at ambient temperature (Requejo *et al*., 2019) and it further confirmed the successful doping of iodine with gold nanoparticle. This also corroborates with the outcome of (Requejo *et al*., 2019) who obtained diffuse concentric rings of gold nanoprism due to the effect of iodide. While in plate VII (c), the SAED pattern reveals bright concentric rings from inner to outer plane with discrete spots (atoms) which are dispersed on the rings. This indicate the polycrystallinity of the Au-I/honeyNCs and it also evidence of successful doping of gold nanoparticle with iodine and honey. It is evident that the amorphous effect of iodine on gold nanoparticle may have been suppressed by honey thereby causing the emerging Au-I/honeyNCs to become polycrystalline. A typical high-resolution image with distinct lattice fringes that had a 0.24 nm spacing was continually viewable. In

light of this, it can be seen that the (111) plane is the preferred location for Au nanoparticle formation. The inter-planar distance of the Au (111) plane agrees with the d-spacing of Au nanoparticles as reported by Zhang *et al.* (2020). The resulting nanoparticles are extremely crystalline, as evidenced by the distinct lattice fringes in the high-resolution image and the selected area electron diffraction (SAED) pattern with bright circular rings corresponding to the (111), (200), (220) and (311) planes.

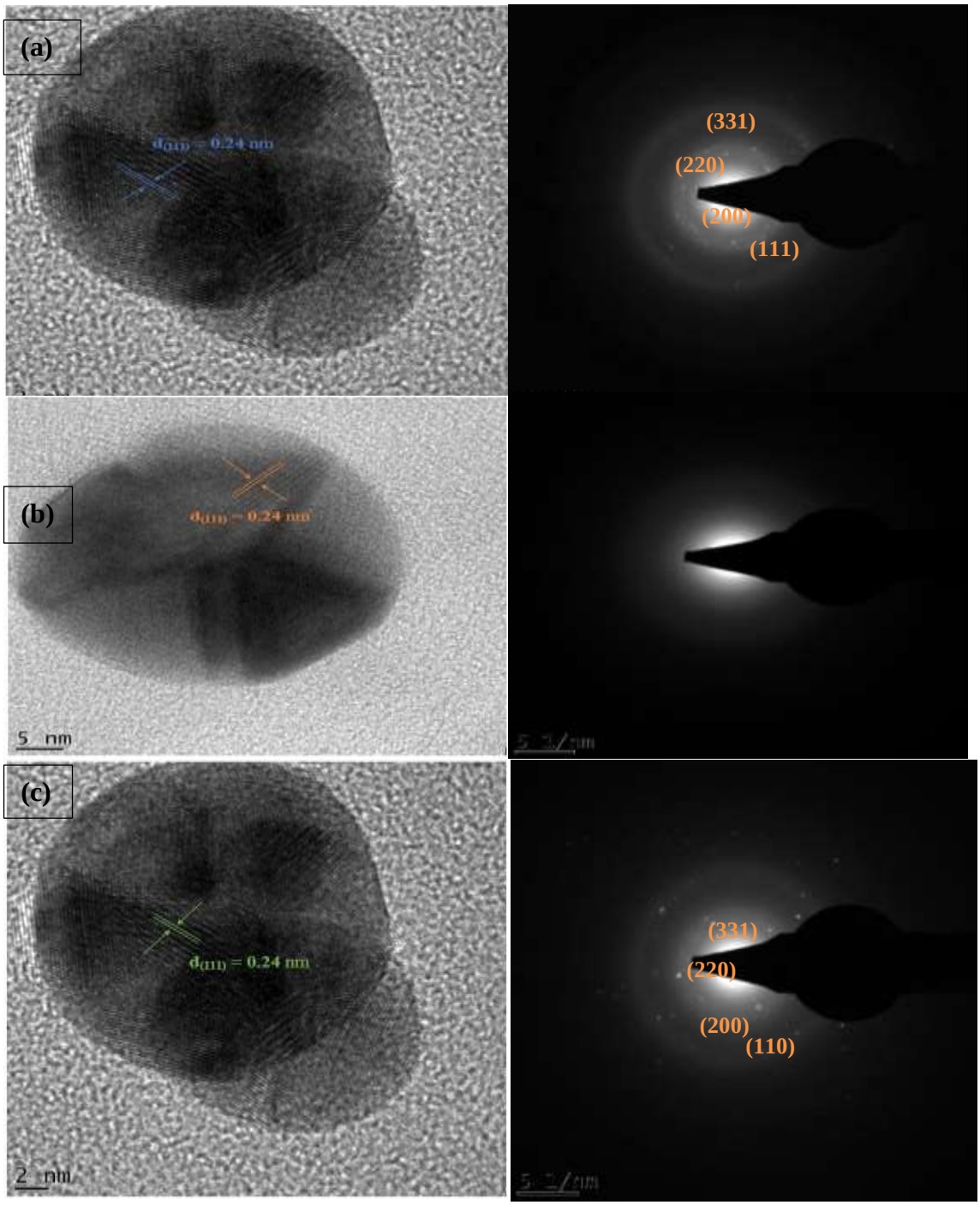

Plate VII (a, b and c): SAED pattern of (a) Au-honeyNCs (b) Au-INCs (c) AuI/honeyNCs

4.5 Energy Dispersive X-ray (EDX) Spectroscopy of Gold Based Nanocomposites The elemental composition of Au-honeyNCs, Au-INCs and Au-I/honeyNCs was further investigated using EDX as shown in Figure 4.4(a, b and c). The EDX spectrum of

AuhoneyNCs in Figure 4.4a confirms the presence of gold with no contamination however the intensity of carbon was high due to the presence of honey and also possibly that of the carbon grid used during the EDX analysis as shown in Figure 4.4a. The vertical axis shows the number of X-ray count and the horizontal axis depicts energy in KeV. The area profile of gold-honey nanocomposite shows peaks gold and carbon which correspond to atomic weight percent of 18.75% and 45.51% respectively. The presence of oxygen signal (35.42%) was also observed which may be due to phenolic group present in the plant extract.

In Figure 4.4b, the area profile of gold-iodine nanocomposite shows several peaks of gold and iodine confirming the formation of gold-iodine nanocomposite. The atomic weight percent of gold and iodine are 26.53% and 15.60% respectively, while carbon has an atomic weight percent of 35.84%. The intensity of carbon peak reduced compared to Figure 4.4a because honey was not included. The presence of oxygen (21.78%) signal was also observed. The carbon emanates as a result of carbon grid utilized for the EDX analysis and possible occurrence along with oxygen from the plant extract used for the gold nanoparticle synthesis. Trace amount of chlorine (0.32%) emanated from the gold salt precursor. The elemental composition of the synthesised gold-iodine nanocomposite supported on honey shown in Figure 4.4c, clearly reveals several peaks of gold and iodine having atomic weight percent of 24.42% and 7.58% respectively while carbon has atomic weight percent of 42.63. The intensity of carbon was high due to the presence of honey (source of carbon) and carbon grid used. Oxygen and chlorine peaks were also observed having atomic weight percent of 25.20% and 0.17% respectively. The trace amount of chlorine may be due to the chloride in the gold salt precursor, while the oxygen may be from the plant extract and other functional

groups in honey used as stabilizer. The EDX result shows that a high purity Au-I/honeyNCs was synthesised.

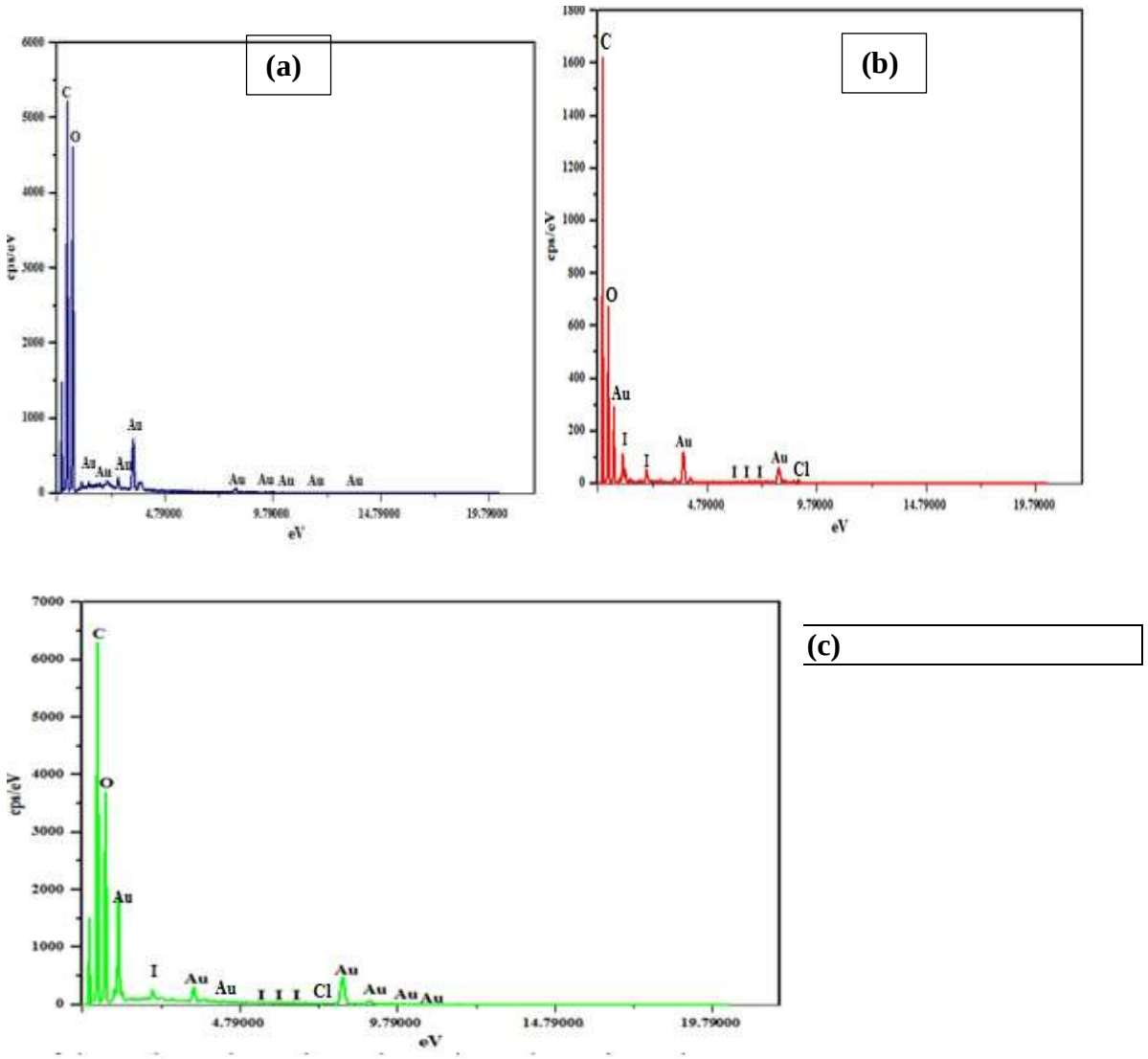

Figure 4.4(a, b and c): Energy Dispersive X-ray Spectrum of (a) Au-honeyNCs (b) Au-INCs (c) Au-I/honeyNCs

4.6 Uncontrolled Release of Iodine on *Staphylococcus aureus, Pseudomonas aeruginosa* and *Escherichia coli*

In-vitro cumulative uncontrolled release profile of povidone iodine on the selected bacteria media was carried out using dialysis bag method and the result is shown in Figure 4.5(a, b and c). From Figure 4.5a, it was noticed that at 20 mins, about 95% of the iodine is already

released on *Staphylococcus aureus*, while about 88% and 77% of the iodine was released on *Escherichia coli* and *Pseudomonas aeruginosa* at 20 mins. This rapid release of iodine on the selected bacteria media is known as "initial burst" release. This initial burst could cause the active agent to be rapidly absorbed or rapidly eliminated. Thus, the active agent spent a limited time in the therapeutic range. Therefore, frequent repetitive dosing may be necessary in order to maintain the therapeutic efficacy of the active agent. This result corroborate to the finding of Fan *et al*. (2019), of an initial burst release of about 87% of free edaravone in the first 30 minutes of reaction time. This observation may be due to the absence of a delivery vehicle (nanocomposite) in both iodine and edaravone.

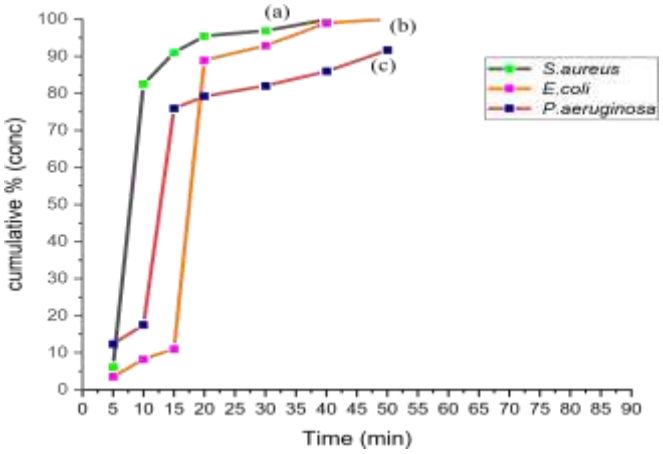

Figure 4.5:- *In-vitro* release profile of iodine on different bacteria media at 35 ^{o}C, pH 5 and stirring speed 120 rpm: (a) *Staphylococcus aureus* (b) *Escherichia coli* (c) *Pseudomonas aeruginosa*

4.7 *In-vitro* Release of Au-INCs

In-vitro cumulative release profile of gold-iodine nanocomposite in different cultured bacterial media (*Staphylococcus aureus, Pseudomonas aeruginosa* and *Escherichia coli*) were carried out using dialysis bag method. Percentage drug release formulation is shown in

Figure 4.6. The sustained drug release rate lasted for 180 mins in the bacteria media over the range of 5-180 min.

Figure 4.6 (a and b) shows the release profile of Au-INCs on *Pseudomonas aeruginosa* and *Escherichia coli* (gram negative bacteria), which clearly reveals that at 180 mins the maximum cumulative concentration (C_{max}) of Au-INCs released was 68.72% and 67.06% on *Pseudomonas aeruginosa* and *Escherichia coli* respectively. This slow release of AuINCs on these bacteria (gram-negative) may be due to the thin cell wall of the bacteria thereby preventing swift penetration of the antibiotic (Au-INCs) on them. Gram-negative bacteria have the ability to identify antibiotic easily and can fight back (Breijyeh *et al*., 2020).

Once the composite material contacted the *Staphylococcus aureus*, within the first 40 mins dissolution and diffusion occurred and the release process commenced swiftly. This may be as result of the small particle size of Au-INCs in contact with the large cell walls of *Staphylococcus aureus* (gram positive bacteria) leading to a slow dissolution rate. The release profile of Au-INCs on *Staphylococcus aureus* as shown in Figure 4.6(c) clearly reveals that at 180 mins the release ratio of the nanocomposite achieved maximum cumulative concentration (C_{max}) of 73.57 %. However, over the range of 120 – 180 mins, the drug release rate was moderate. This may be as a result of the suppressive influence of the nanocomposite on the bacteria. *Staphylococcus aureus* being a gram- positive bacteria are more susceptible to antibiotic due to their larger cell wall and can easily absorbed antibiotic (Breijyeh *et al*., 2020). Small size metallic nanocomposite (Au-INCs) allow them to have sufficient contact with large surface bacteria leading to a high release rate on the bacteria.

Although this result does not corroborate to the findings of Fan *et al*., (2019), who achieved 83% of edavarone released from edavarone nanocomposite hydrogel in the first 3 hours of

the reaction. This may be likened to the disparity in nanocomposite materials and reaction media.

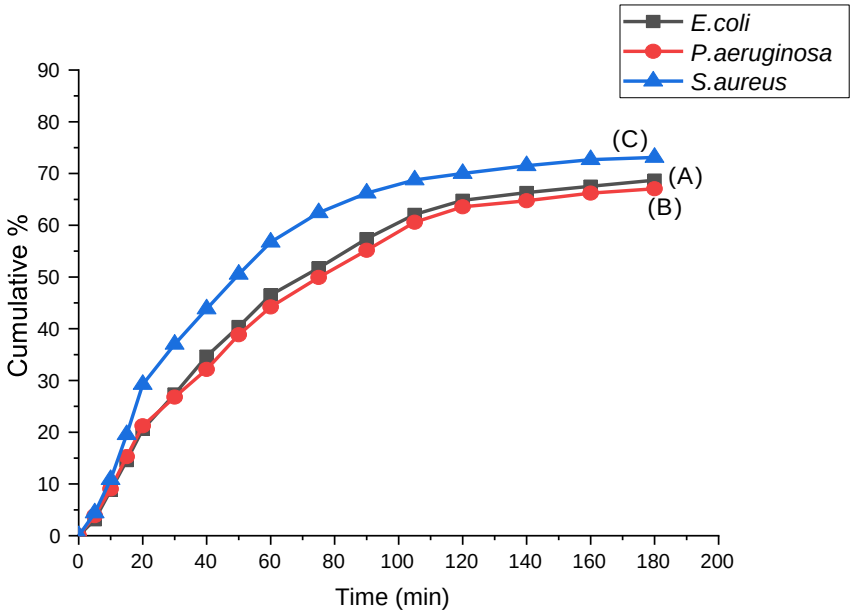

Figure 4.6: - *In-vitro* release profile of Au-INCs on different bacteria media at 35 ^{o}C, pH 5 and stirring speed of 120 rpm: (a) *Escherichia coli* (b) *Pseudomonas aeruginosa* (c) *Staphylococcus aureus*

4.8 *In-vitro* Release of Au-I/honeyNCs

The *in-vitro* release of Au-I/honeyNCs was investigated in three different bacteria media (*Pseudomonas aeruginosa, Staphylococcus aureus* and *Escherichia coli*). It was evident that the release behavior of Au-I/honeyNCs matrix increases in these bacteria media (*Pseudomonas aeruginosa, Staphylococcus aureus* and *Escherichia coli*) compare to AuINCs as shown in Figure 4.7. The sustained drug release rate from Au-I/honeyNCs lasted for 180 mins and the drug release rate accelerated and release amount of 96.91% was achieved for *Escherichia coli*, 97.62% for *Pseudomonas aeruginosa* and 99.54% was

achieved for *Staphylococcus aureus*. The fast release/diffusion of Au-I/honeyNCs may be due to the polycrystalline structure of the nanocomposite and also the large particle size of Au-I/honeyNCs which may have prompted a controlled release of Au-I/honeyNCs. Heavier particles will move slowly and so will have a slower rate of diffusion thereby having sufficient effect/contact on the bacteria cell wall which may have degrade the cell wall rapidly.

The release profile of Au-I/honeyNCs on *Staphylococcus aureus* as shown in Figure 4.7a, clearly reveals that at 180 mins the release ratio of the drug achieved maximum cumulative concentration (C_{max}) of 99.54%. This may be linked to the large particle size of AuI/honeyNCs which may have prompted fast degradation of the cell wall of *Staphylococcus aureus*. However, over the range of 120 – 180 mins, the drug release rate was stable. The diffusion of active agent depends solemnly on the matrix structure (Panotopoulos and Haidar, 2019). While for *Pseudomonas aeruginosa* and *Escherichia coli* the maximum concentration achieved at 180 min were 97.62% and 96.91% respectively. These variation in the amount of drug release may be due to the insusceptibility of gram-negative bacteria to antibiotic. *Staphylococcus aureus* being a gram- positive bacteria are more susceptible to antibiotic due to their larger cell wall can easily absorbed antibiotic (Breijyeh *et al*., 2020). Similar trend has been reported by Gao *et al.* (2018) on the delivery of deferoxamine and hydroxysafflor yellow A to accelerate diabetic wound healing. In Figure 4.7, it shows that as the amount of Au-I/honeyNCs released on the bacteria media increases in function of time. This implies the rate of dissolution/diffusion as well as release rate was higher. This may have prompted effective concentration of the composite on the bacteria media which may tends to degrade the bacteria rapidly. Generally, the release of active compound from its matrix is a function

of several factors such as diffusion, partitioning, osmosis, swelling and erosion (Permanadewi *et al*., 2019).

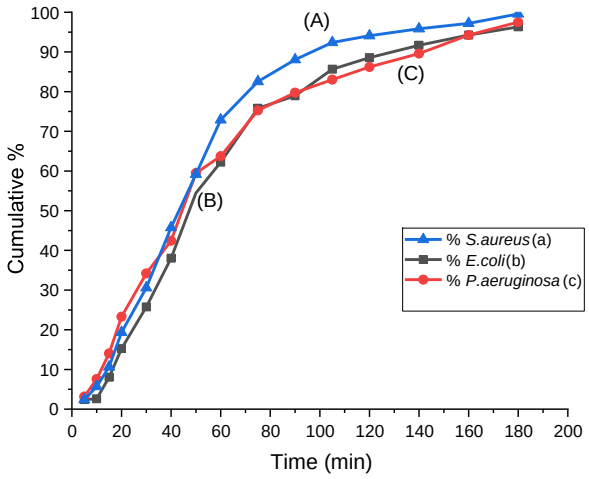

Figure 4.7:- *In-vitro* release profile of iodine from Au-I/honeyNCs in different bacteria media at 35 ^{o}C, pH 5 and stirring speed 120 rpm: (a) *Staphylococcus aureus* (b) *Escherichia coli* (c) *Pseudomonas aeruginosa*

4.9 Kinetic release model of Au-INCs and Au-I/honeyNCs on the Bacteria

The release profiles Au-INCs and Au-I/honeyNCs in the bacteria media were analyzed by fitting the obtained release data to different kinetic models, which were the zero order, first order, Higuchi, and Korsmeyer-Peppas models to obtain insights into the mechanism of the release.

Modeling Kinetic	***S. aureus***	***P. aureginosa***	***E. coli***
Zero order release			
R_2	0.935	0.714	0.788
K_0	5.1×10^{-2}	3.1×10^{-2}	3.5×10^{-2}
χ^2	0.0310	0.0521	0.0493
MSE	0.0042	0.0105	0.0086
First order release			
R^2	0.957	0.867	0.909
K_1	5.8×10^{-3}	4.1×10^{-3}	4.6×10^{-3}
χ^2	0.0282	0.0336	0.0303
MSE	0.0039	0.0092	0.0080
Higuchi Model			
R_2	0.966	0.883	0.916
K_H	7.53×10^{-1}	4.9×10^{-1}	5.5×10^{-1}
χ^2	0.0251	0.0347	0.0282
MSE	0.0028	0.0088	0.0079
Kosmeryer-peppas Model			
R_2	0.864	0.896	0.889
K_{kp}	5.3×10^{-2}	4.3×10^{-1}	4.6×10^{-1}

N	0.47	0.556	0.554	**4.9.1**
χ^2	0.0334	0.0311	0.0326	

Interpretation of R^2 value and rate constant of release kinetics of Au-INCs The results of the release kinetic of Au-INCs in *Staphylococcus aureus*, *Pseudomonas aeruginosa* and *Escherichia coli* are summarized in Table 4.2 and all graphical plots are shown in the appendix page of this thesis (Appendix A, B and C). **Table 4.2: Kinetic release of Au-INCs on Different Bacteria**

MSE	0.0118	0.0103	0.0108

From the table 4.2, R^2 is the correlation value, K_{kp} is rate constant and n is release exponent. In order to select a model that best fits the experimental data, Chi-square (χ^2) and the mean square error (MSE) presented in Tables 4.2 and 4.3 were used to justify the favoured kinetic model. The smaller the error value, the closer the agreement in the fit between the experimental data of the kinetic equations using the following relationships in equations 4.1 and 4.2:

$$\chi^2 = \sum_{i=1} \frac{(q_{e,exp} - q_{e,cal})}{q_{e,cal}} \quad (4.1)$$

$$MSE = \frac{1}{} \sum_{i=1n}^{n} \quad (q_{e,exp} - q_{e,cal})^2 \quad (4.2)$$

The release profile of Au-INCs on the bacteria media was studied using different kinetic models. The model that best describe the release profile of Au-INCs on the bacteria is chosen based the highest R^2 and MSE. The Higuchi release model has the following R^2 value; 0.966, 0.883 and 0.916 of Au-INCs release profile on *Staphylococcus aureus*, *Pseudomonas aeruginosa* and *Escherichia coli* respectively as shown in Table 2. The release profile of Au-INCs shows a best fit to Higuchi release model on the selected bacteria based on its highest R^2 value and mean square error (MSE). This implies that the diffusivity of Au-INCs is constant during the predetermine application and the drug matrix do no swell upon contact with the bacteria media (Peppas, 2019).

Furthermore, the Kosmeryer-peppas model is used as a decision parameter to determine the mechanism of Au-INCs release on the selected bacteria based on the release exponent (n) value. From Table 4.2, the following release exponent value 0.47, 0.556 and 0.554 of AuINCs on *Staphylococcus aureus*, *Pseudomonas aeruginosa* and *Escherichia coli*

respectively. This implies that the magnitude of release exponent n indicates the release mechanism of Au-INCs on *staphylococcus aureus* is Fickian diffusion while on *Pseudomonas aeruginosa* and *Escherichia coli* are non-fickian diffusion.

4.9.2 Interpretation of R^2 value and rate constant of release kinetics of Au-I/honeyNCs

The results of the release kinetic of Au-I/honeyNCs in *Staphylococcus aureus*, *Pseudomonas aeruginosa* and *Escherichia coli* are summarized in Tables 4.3 and all graphical plots are shown in the appendices pages of this thesis (Appendices D, E and F).

Table 4.3: Kinetic release of Au-I/honeyNCs on different bacteria.

Modeling Kinetic	***S. aureus***	***P. aeruginosa***	***E. coli***
Zero order release			
R_2	0.984	0.914	0.917
K_0	8.6×10^{-2}	7.1×10^{-2}	8.1×10^{-2}
χ^2	0.295	0.281	0.276
MSE	0.0201	0.0182	0.0174
First order release			
R^2	0.963	0.787	0.886
K_1	6.3×10^{-3}	3.8×10^{-3}	5.1×10^{-3}
χ^2	0.316	0.477	0.390
MSE	0.0253	0.0358	0.0322
Higuchi Model			
R_2	0.913	0.815	0.877
K_H	1.2098	9.76×10^{-1}	1.134
χ^2	0.340	0.441	0.407

R_2	0.85	0.851	0.865
K_{kp}	5.8×10^{-1}	4.4×10^{-1}	5.2×10^{-1}
N	0.663	0.585	0.849
χ^2	0.492	0.478	0.469
MSE	0.180	0.178	0.165
MSE	0.211	0.256	0.238
Kosmeryer-peppas Model			

From table 4.3, the release profile of Au-I/honeyNCs shows a best fit to zero order release model on the three bacteria media based on its highest (R^2) correlation value and MSE; 0.984, 0.914 and 0.917 on *Staphylococcus aureus, Pseudomonas aeruginosa* and *Escherichia coli* respectively. This implies that the concentration of Au-I/honeyNCs is uniform on the selected bacteria over the predetermine time of application. Transdermal drug delivery system always fit into zero order release model (Peppas, 2019).

Finally, the Kosmeryer-peppas model is used to determine the mechanism of the release based on the release exponent value. The following release exponent 0.663, 0.585 and 0.849 of Au-I/honeyNCs on *Staphylococcus aureus, Pseudomonas aeruginosa* and *Escherichia coli* respectively as shown in Table 4.3. The magnitude of the release exponent n indicates that the release mechanism of Au-I/honeyNCs is non-fickian diffusion.

CHAPTER FIVE

5.0 CONCLUSION AND RECOMMENDATIONS

5.1 Conclusion

This study focused on the preparation of AuNPs, Au-INCs, and Au-INCs supported on natural honey and evaluation of its delivery on selected strains of bacteria present in open wound treatment. AuNPs were synthesised via green route using *Agerantum conyzoides* plant extract to reduce the gold precursor salt. Au-INCs and Au-I/honeyNCs were synthesised using wet impregnation and ultra sonication methods. The developed nanocomposite (Au-INCs and Au-I/honeyNCs) were characterised and delivered to the cultured bacteria media using dialysis bag method in order to improve the efficacy of the incorporated active agents in the nanocomposite over the therapeutic range. Furthermore, the release mechanism of Au-INCs and Au-I/honeyNCs were investigated using zero order release model, first order release model, Higuchi model and Kosmeyer-peppas release model. Based on the obtained result the following conclusions were drawn:

i. The qualitative phytochemical results indicated that the plant extract and honey are rich in secondary metabolites such as phenols, saponins, flavonoids and tannins.

ii. The biosynthesized AuNPs and functionalization of Au/Idoine/honey were characterised using various analytical instruments. UV-Visible spectroscopy shows the surface plasmon resonance (SPR) peak at 548nm, HRTEM shows

the spherical and quasi-spherical shapes of AuNPs, Au/honeyNCs, Au-INCs and Au-I/honeyNCs which were uniformly distributed with an average

particle size of 13.08, 14.97, 32.60 nm and 37.57 nm respectively. The SAED pattern of Au-I/honeyNCs shows a polycrystalline structure, while Au-INCs is amorphous. The EDX reveals the synthesised nanocomposites are of high purity.

iii. The *In-vitro* release profile of Au-INCs shows that the cumulative maximum concentration (C_{max}) released on *Staphylococcus aureus, Pseudomonas aeruginosa* and *Escherichia coli* were 73.57%, 68.72% and 67.06% respectively over the time frame of 180 minutes.

iv. The *In-vitro* release profile of Au-I/honeyNCs reveals the cumulative maximum concentration (C_{max}) released on *Staphylococcus aureus, Pseudomonas aeruginosa* and *Escherichia coli* were 99.54%, 97.62% and 96.91% respectively over the time frame of 180 minutes.

v. The kinetic model shows that Au-INCs is best fitted to Higuchi model based on its highest (R^2) correlation value and mean square error (MSE). Kosmeryer-peppas model reveals that the mechanism of release of Au-INCs is both fickian and non-fickian diffusion on the selected bacteria.

vi. Au-I/honeyNCs release profile shows an excellent fit to zero order release model on all the selected bacteria. Thus, Au-I/honeyNCs is most suitable for transdermal system. Kosmeryer-peppas model reveals that the mechanism of release of Au-I/honeyNCs is non-fickian diffusion on the selected bacteria.

5.2 Recommendations

Based on the outcome of this present study, further studies should be carried out on the following areas;

I. The toxicity level of the synthesised Au-INCs and Au-I/honeyNCs on human skin especially for application in open wound treatment.

II. Optimization of the process conditions of the synthesised Au-INCs and Au-I/honeyNCs.

III. Clinical trials should be carried out on the synthesised nanocomposites for possible commercialization.

5.3 Suggestions for further study

In addition, further research is needed in the following areas;

I. *In-vivo* assessment of the nanocomposite materials (Au-INCs and Au-I/honeyNCs) for controlled transdermal drug delivery should be studied.

II. Other transition metals that are cost effective and biocompatible should be evaluated as a possible substitute for the gold nanocomposite materials.

5.4 Contributions to Knowledge

In this study, 50 cm^3 of AuNPs were functionalized with 10 cm^3 of povidone iodine solution and natural honey to produce two nanocomposite materials: Au-INCs and AuI/honeyNCs, which are effective against *Staphylococcus aureus*, *Pseudomonas aeruginosa*, and *Escherichia coli* bacteria in open wounds. *In-vitro* delivery of Au-INCs revealed cumulative maximum concentrations (C_{max}) of 73.57%, 68.72%, and 67.06% released on *Staphylococcus aureus, Pseudomonas aeruginosa,* and *Escherichia coli,* respectively, over a time frame of 180 minutes. While Au-I/honeyNCs revealed the cumulative maximum concentrations of

99.54%, 97.62%, and 96.91% released on *Staphylococcus aureus, Pseudomonas aeruginosa*, and *Escherichia coli*, respectively, over the time frame of 180 minutes. The diffusion exponent (n) values of Au-INCs were 0.47, 0.556 and 0.554 on *Staphylococcus aureus*, *Pseudomonas aeruginosa* and *Escherichia coli* respectively. This implies that the mechanism of delivery of Au-INCs on *staphylococcus aureus* was influenced by Fickian diffusion (i.e $n \leq 0.5$) and non-fickian diffusion (i.e $n > 0.5$) for *Pseudomonas aeruginosa* and *Escherichia coli*. While the diffusion exponent (n) values of Au-I/honeyNCs were 0.663, 0.585 and 0.849 on *Staphylococcus aureus, Pseudomonas aeruginosa* and *Escherichia coli* respectively. This implies that the mechanism of delivery of Au-I/honeyNCs was influenced strictly by non-fickian diffusion (i.e $n > 0.5$).

REFERENCES

Abbas, M., Shah, I., Nawaz, M. A., Pervez, S., Hussain, Y., Niaz, K., & Khan, F. (2021). Honey Against Cancer. *Nutraceuticals and Cancer Signaling: Clinical Aspects and Mode of Action*, 401-418.

Abdullahi, R., & Hamza, A. B. (2020). Physiological Roles of Phenolic Compounds Isolated from Medicinal Plants of Tropical Origin. *International Journal Of Science for Global Sustainability*, 6(4), 133-143.

Adelakun, S. A., Ogunlade, B., Omotoso, O. D., & Oyewo, O. O. (2018). Response of Crude Leaf Extract of Ageratum conyzoides on Hormonal and Biochemical assay in Streptozotocin induced Diabetics male wistar rats. *Indian Journal Pharmacol*, 62(4), 413-423.

Adesanwo, J. K., Egbomeade, C. O., Moronkola, D. O., & Akinpelu, D. A. (2019). Chemical, toxicity and antibacterial studies on methanol extracts of Melanthera scandens, Ageratum conyzoides, Aspilia Africana and Synedrella nodiflora. *Journal of Exploratory Research in Pharmacology*, 4(1), 1-7.

Ailincai, D., Gavril, G., & Marin, L. (2020). Polyvinyl alcohol boric acid–A promising tool for the development of sustained release drug delivery systems. *Materials Science and Engineering*, 107, 110316.

Akturk, O., Kismet, K., Yasti, A. C., Kuru, S., Duymus, M. E., Kaya, F. & Keskin, D. (2016). Collagen/gold nanoparticle nanocomposites: a potential skin wound healing biomaterial. *Journal of Biomaterials Applications*, 31(2), 283-301.

Alam, A., Machale, M. U., Yadav, R. P., Sharma, M., & Patel, A. K. (2021). Role of Transdermal Drug Delivery System. *Asian Journal of Pharmaceutical Research and Development*, 9(3), 137-143.

Aldosari, H. (2022). Graphene Reinforced Polymer Matrix Nanocomposites: Fabrication Method, Properties and Applications. *Journal of Biomaterials Applications*, 3(2), 120-133.

Alotaibi, F. A. (2021). Iodine in a nutshell: what do you need to know? *Journal of Biomaterials Applications*, 983-1087.

Amina, S. J., & Guo, B. (2020). A review on the synthesis and functionalization of gold nanoparticles as a drug delivery vehicle. *International Journal of Nanomedicine*, 9823-9857.

Anjum, S., Komal, A., Abbasi, B. H., & Hano, C. (2021). Nanoparticles as elicitors of biologically active ingredients in plants. *Nanotechnology in Plant Growth Promotion and Protection: Recent Advances and Impacts*, 170-202.

Aragaw, T. A., Bogale, F. M., & Aragaw, B. A. (2021). Iron-based nanoparticles in wastewater treatment: A review on synthesis methods, applications, and removal mechanisms. *Journal of Saudi Chemical Society*, 25(8), 101280.

Argenta, D. F., dos Santos, T. C., Campos, A. M., & Caon, T. (2019). Hydrogel nanocomposite systems: physico-chemical characterization and application for drug-delivery systems. *Nanocarriers for Drug Delivery*, 81-131.

Asiya, S. I., Pal, K., Kralj, S., El-Sayyad, G. S., Souza, F. G., & Narayanan, T. (2020). Sustainable preparation of gold nanoparticles via green chemistry approach for biogenic applications. *Materials Today Chemistry*, 17, 100327.

Aslam, M., Abdullah, A. Z., & Rafatullah, M. (2021). Recent development in the green synthesis of titanium dioxide nanoparticles using plant-based biomolecules for environmental and antimicrobial applications. *Journal of Industrial and Engineering Chemistry*, 98, 1-16.

Association of Official Analytical Chemists. (AOAC). (2002). Official methods of analysis of AOAC International, 15th edition, volume II. (Edited by K. Helich), *AOAC International*. 22201-23301.

Awad, M.A.G., Hendi, A.A., Wagealla, M. A. E., Virk, P., & Ortashi, K. M. O. (2018). Disposable piezoelectric polymer bandage for percutaneous delivery of drugs and method for such percutaneous delivery. *British Journal of Clinical Pharmacy*, 3454.

Bai, X., Yang, Y., Zheng, W., Huang, Y., Xu, F., & Bao, Z. (2023). Synergistic Photothermal Antibacterial Therapy Enabled by Multifunctional Nanomaterials: Progress and Perspectives. *Materials Chemistry Frontiers* 12, 1-16.

Baier, M., & Carmignato, S. (2022). Contrast based method for the automated analysis of transfer functions and spatial resolution limits of micro-and nano-focus computed tomography systems: Evaluation with simulated data. *Optics and Lasers in Engineering*, 157, 107113.

Banerjee, P., & Qamar, I. (2022). Nanobiomaterials in biomedicine: Designing approaches and critical concepts. *Nanobioanalytical Approaches to Medical Diagnostics*, 345361.

Bharadwaj, K. K., Rabha, B., Pati, S., Sarkar, T., Choudhury, B. K., Barman, A., & Mohd Noor, N. H. (2021). Green synthesis of gold nanoparticles using plant extracts as beneficial prospect for cancer theranostics. *Molecules*, 26(21), 6389.

Bigliardi, P., Langer, S., Cruz, J. J., Kim, S. W., Nair, H., & Srisawasdi, G. (2017). An Asian perspective on povidone iodine in wound healing. *Dermatology*, 233(3), 223233.

Bohrey, S., Chourasiya, V., & Pandey, A. (2016). Polymeric nanoparticles containing diazepam: preparation, optimization, characterization, in-vitro drug kinetic study. *Nano Convergence*, 3(1), 1-7.

Breijyeh, Z., Jubeh, B., & Karaman, R. (2020). Resistance of Gram-negative bacteria to current antibacterial agents and approaches to resolve it. *Molecules*, 25(6), 1340.

Bruschi, M. L. (2018). Mathematical models of drug release: Strategies to Modify the Drug Release from Pharmaceutical Systems. *International Journal of Nanomedicine*, 5(2), 2-15.

Bukhari, A., Ijaz, I., Gilani, E., Nazir, A., Zain, H., Saeed, R., & Naseer, Y. (2021). Green synthesis of metal and metal oxide nanoparticles using different plants' parts for antimicrobial activity and anticancer activity: a review article. *Coatings*, 11(11), 1374.

Chahal, R., Nanda, A., Akkol, E. K., Sobarzo-Sánchez, E., Arya, A., Kaushik, D., & Mittal, V. (2021). Ageratum conyzoides L. and its secondary metabolites in the management of different fungal pathogens. *Molecules*, 26(10), 2933.

Chander, S., Piplani, M., Waghule, T., & Singhvi, G. (2022). Role of chitosan in transdermal drug delivery. *Chitosan in Drug Delivery*, 83-105.

Chandrakala, V., Aruna, V., & Angajala, G. (2022). Review on metal nanoparticles as nanocarriers: Current challenges and perspectives in drug delivery systems. *Emergent Materials*, 1-23.

Cheesbrough, M. (2005). District laboratory practice in tropical countries, part 2. Cambridge university press. 234-453.

Das, J., Debbarma, A. N. I. M. A., & Lalhlenmawia, H. (2021). Formulation and in vitro evaluation of poly-(D, L-lactide-co-glycolide)(PLGA) nanoparticles of ellagic acid and its effect on human breast cancer, MCF-7 cell line. *International Journal of Nanomedicine*, 13, 56-62.

Davane, M., Rao, A., & Nagoba, B. (2019). The safety and efficacy of commonly used topical agents in the treatment of wound infections. *Wound Healing Southern Africa*, 12(1), 34-37.

De, A., Singh, N. B., Guin, M., & Barthwal, S. (2023). Water purification by green synthesized nanomaterials. *Current Pharmaceutical Biotechnology*, 24(1), 101-117.

Dongare, A., Jagtap, A., Bhise, R., Shaikh, A., Ingale, S., & Kakad, S. (2019). Physicochemical characterization and membrane stabilizing activity of different honey samples: A comparative study. *Asian Journal of Pharmacy and Pharmacology*, 5(2), 373-377.

Duan, Y., Dhar, A., Patel, C., Khimani, M., Neogi, S., Sharma, P., & Vekariya, R. L. (2020). A brief review on solid lipid nanoparticles: Part and parcel of contemporary drug delivery systems. *RSC Advances*, 10(45), 26777-26791.

Edis, Z., Haj Bloukh, S., Abu Sara, H., Bhakhoa, H., Rhyman, L., & Ramasami, P. (2019). "Smart" triiodide compounds: Does halogen bonding influence antimicrobial activities? *Pathogens*, 8(4), 182.

El-Hamshary, H., El-Newehy, M. H., Abdulhameed, M. M., El-Faham, A., & Elsherbiny, A. S. (2019). Evaluation of clay-ionene nanocomposite carriers for controlled drug delivery: Synthesis, in vitro drug release, and kinetics. *Materials Chemistry and Physics*, 225, 122-132.

El-Kheir, A., & El-Gabry, L. K. (2022). Potential Applications of Nanotechnology In Functionalization of Synthetic Fibres (A Review). *Egyptian Journal of Chemistry*, 65(7), 57-84.

Emam-Ismail, M., El-Hagary, M., Shaaban, E. R., Moustafa, S. H. & Gad, G. M. A. (2019). Spectroscopic ellipsometry and morphological characterizations of nanocrystalline Hg1-xMnxO oxide diluted magnetic semiconductor thin films. *Ceramics International*, 45(7), 8380-8387.

Enrico, C. (2019). Nanotechnology-based drug delivery of natural compounds and phytochemicals for the treatment of cancer and other diseases. *Studies in Natural Products Chemistry*, 62, 91-123.

Eshgh, N. A., Meftahi, A., Khajavi, R., Aljabali, A. A., & Barhoum, A. (2022). Nanocelluloses for tissue engineering and biomedical scaffolds. *Egyptian Journal of Chemistry*, 61(9), 67-85.

Fan, Y., Wu, W., Lei, Y., Gaucher, C., Pei, S., Zhang, J., & Xia, X. (2019). Edaravoneloaded alginate-based nanocomposite hydrogel accelerated chronic wound healing in diabetic mice. *Marine Drugs*, 17(5), 285.

Fathil, M. A. M., Taufeq, F. Y. F., Abdalla, S. S. I., & Katas, H. (2022). Roles of chitosan in synthesis, antibacterial and anti-biofilm properties of bionano silver and gold. *RSC Advances*, 12(30), 19297-19312.

Gao, S. Q., Chang, C., Li, J. J., Li, Y., Niu, X. Q., Zhang, D. P., ... & Gao, J. Q. (2018). Codelivery of deferoxamine and hydroxysafflor yellow A to accelerate diabetic wound healing via enhanced angiogenesis. *Drug Delivery*, 25(1), 1779-1789.

Garanti, T., Alhnan, M. A., & Wan, K. W. (2021). The potential of nanotherapeutics to target brain tumors: current challenges and future opportunities. *Current Pharmacuetical Design*, 12-35.

Gholipourmalekabadi, M., Mobaraki, M., Ghaffari, M., Zarebkohan, A., Omrani, V. F., Urbanska, A. M., & Seifalian, A. (2017). Targeted drug delivery based on gold nanoparticle derivatives. *Current Pharmaceutical Design*, 23(20), 2918-2929.

Ghramh, H. A., Ibrahim, E. H., & Ahmad, Z. (2021). Antimicrobial, immunomodulatory and cytotoxic activities of green synthesized nanoparticles from Acacia honey and Calotropis procera. *Saudi Journal of Biological Sciences*, 28(6), 3367-3373.

Gmur, M. K., & Karpiński, T. M. (2020). Povidone-iodine in wound healing and prevention of wound infections. *European Journal of Biological Research*, 10(3), 232-239.

Gomathi, A. C., Rajarathinam, S. X., Sadiq, A. M., & Rajeshkumar, S. (2020). Anticancer activity of silver nanoparticles synthesized using aqueous fruit shell extract of Tamarindus indica on MCF-7 human breast cancer cell line. *Journal of Drug Delivery Science and Technology*, 55, 101376.

Gomez, T. W., Gomez, J. W., & Gopal, R. (2020). Clinical Applications and Benefits of Using Closed-Incision Negative Pressure Therapy for Incision and Surrounding Soft Tissue Management: A Novel Approach for Comorbid Wounds. *Cureus*, 12(7), 315.

Gulati, S., Kumar, S., Singh, P., Diwan, A., & Mongia, A. (2021). Biocompatible chitosancoated gold nanoparticles: novel, efficient, and promising Nanosystems for Cancer treatment. *Handbook of Polymer and Ceramic Nanotechnology*, 811-838.

Haidari, H., Melguizo-Rodríguez, L., Cowin, A. J., & Kopecki, Z. (2023). Therapeutic potential of antimicrobial peptides for treatment of wound infection. *American Journal of Cell Physiology*, 324(1), C29-C38.

Hammami, I., & Alabdallah, N. M. (2021). Gold nanoparticles: Synthesis properties and applications. *Journal of King Saudi University Science*, 33(7), 101560.

Harborne, J. B. (1998). Phytochemical Methods. A Guide to Modern Techniques of Plant Analysis. *General Pharmacology*, 31 (4), 601-606.

Hariani, N., Mismawati, A., & Ruga, R. (2022). Phytochemical Analysis of Ethanol Extract from Stingless Bee (Tetragonula laeviceps Smith) Honey and Its Anti-Acnes Activity. *International Conference on Tropical Studies (ICTROPS)*, 1(1), 101-107.

Hassan, H., Sharma, P., Hasan, M. R., Singh, S., Thakur, D., & Narang, J. (2022). Gold nanomaterials–The golden approach from synthesis to applications. *Materials Science for Energy Technologies*, 12-18.

Herdiana, Y., Wathoni, N., Shamsuddin, S., Joni, I., & Muchtaridi, M. (2021). ChitosanBased Nanoparticles of Targeted Drug Delivery System in Breast Cancer Treatment. *Polymers*, 13(11), 1717.

Hernández-Rangel, A., & Martin-Martinez, E. S. (2021). Collagen based electrospun materials for skin wounds treatment. *Journal of Biomedical Materials Research Part A*, 109(9), 1751-1764.

Hussein, M. A. M., Ulag, S., Dena, A. S. A., Sahin, A., Grinholc, M., Gunduz, O., & Megahed, M. (2021). Chitosan/gold hybrid nanoparticles enriched electrospun PVA nanofibrous mats for the topical delivery of Punica granatum L. extract: synthesis, characterization, biocompatibility and antibacterial properties. *International Journal of Nanomedicine*, 16, 5133.

Jakubowicz, I., Enebro, J., & Yarahmadi, N. (2021). Challenges in the search for nanoplastics in the environment: A critical review from the polymer science perspective. *Polymer Testing*, 93, 106953.

Jaldin, C. L., Silva, N., & Martínez, J. (2022). Nanomaterials Based on Honey and Propolis for Wound Healing: A mini-Review. *Nanomaterials*, 12(24), 4409.

John, T., Gladytz, A., Kubeil, C., Martin, L. L., Risselada, H. J., & Abel, B. (2018). Impact of nanoparticles on amyloid peptide and protein aggregation: a review with a focus on gold nanoparticles. *Nanoscale*, 10(45), 20894-20913.

Kanapathy, M., Hachach, H. N., Bystrzonowski, N., Connelly, J. T., O'Toole, E. A., Becker, D. L., & Richards, T. (2017). Epidermal grafting for wound healing: a review on the harvesting systems, the ultrastructure of the graft and the mechanism of wound healing. *International Wound Journal*, 14(1), 16-23.

Khan, S., & Hossain, M. K. (2022). Classification and properties of nanoparticles. In *Nanoparticle-based Polymer Composites*, 15-54.

Kim, H.S., Sun, X., L. J. H., Kim, H. W., Fu, X., & Leong, K. W. (2019). Advanced drug delivery systems and artificial skin grafts for skin wound healing. *Advanced Drug Delivery Reviews*, 146, 209-239.

Kisiriko, M., Anastasiadi, M., Terry, L. A., Yasri, A., Beale, M. H., & Ward, J. L. (2021). Phenolics from medicinal and aromatic plants: Characterisation and potential as biostimulants and bioprotectants. *Molecules*, 26(21), 6343.

Kolimi, P., Narala, S., Nyavanandi, D., Youssef, A. A. A., & Dudhipala, N. (2022). Innovative Treatment Strategies to Accelerate Wound Healing: Trajectory and Recent Advancements. *Cells*, 11(15), 2439.

Kumar, P.V., Kala, S.M. J. & Prakash, K. S. (2019). Green synthesis of gold nanoparticle using croton Caudatus Geisel leaf extract and their biology study. *Materials Letters*, 236, 19-22.

Kumar, R., Aadil, K. R., Ranjan, S., & Kumar, V. B. (2020). Advances in nanotechnology and nanomaterials based strategies for neural tissue engineering. *Journal of Drug Delivery Science and Technology*, 57, 101617.

Kumar, S. P., Asokan, Y., Balamurugan, K., & Harsha, B. (2022). A review of wound dressing materials and its fabrication methods: Emphasis on three-dimensional printed dressings. *Journal of Medical Engineering & Technology*, 46(4), 318-334.

Kumari, P. V. K., Rao, Y. S., & Akhila, S. (2019). Role of nanocomposites in drug delivery. *GSC Biological and Pharmaceutical Sciences*, 8(3), 5-23.

Lee, K. X., Shameli, K., Yew, Y. P., Teow, S. Y., Jahangirian, H., Rafiee-Moghaddam, R., & Webster, T. J. (2020). Recent developments in the facile biosynthesis of gold nanoparticles (AuNPs) and their biomedical applications. *International Journal of Nanomedicine*, 275-300.

Lei, W., Yang, C., Wu, Y., Ru, G., He, X., Tong, X., & Wang, S. (2022). Nanocarriers surface engineered with cell membranes for cancer targeted chemotherapy. *Journal of Nanobiotechnology*, 20(1), 1-21.

Li, Q., & Cheng, S. (2020). Polymer nanocomposites for high-energy-density capacitor dielectrics: Fundamentals and recent progress. *IEEE Electrical Insulation Magazine*, 36(2), 7-28.

Li, Q., Lu, F., Zhou, G., Yu, K., Lu, B., Xiao, Y., & Lan, G. (2017). Silver inlaid with gold nanoparticle/chitosan wound dressing enhances antibacterial activity and porosity, and promotes wound healing. *Biomacromolecules*, 18(11), 3766-3775.

Liu, R., Luo, C., Pang, Z., Zhang, J., Ruan, S., Wu, M., & Gao, H. (2022). Advances of nanoparticles as drug delivery systems for disease diagnosis and treatment. *Chinese Chemical Letters*, 20(1), 1-21.

Malaki, M., Xu, W., Kasar, A. K., Menezes, P. L., Dieringa, H., Varma, R. S., & Gupta, M. (2019). Advanced metal matrix nanocomposites. *Metals*, 9(3), 330.

Manju, R., & Savi, D. (2018). Synthesis of Gold Nanoparticles from Natural Honey and its Application in Antifungal Activity. *Journal of Nanobiotechnology*, 2(1), 1-19.

Marofi, F., Alexandrovna, K. I., Margiana, R., Bahramali, M., Suksatan, W., Abdelbasset, W. K., & Maashi, M. S. (2021). MSCs and their exosomes: a rapidly evolving approach in the context of cutaneous wounds therapy. *Stem Cell Research & Therapy*, 12(1), 1-20.

Martinengo, L., Olsson, M., Bajpai, R., Soljak, M., Upton, Z., Schmidtchen, A., & Järbrink, K. (2019). Prevalence of chronic wounds in the general population: systematic review and meta-analysis of observational studies. *Annals of Epidemiology*, 29, 815.

Mehta, M., Keerthy, H. S., & Yadav, R. P. (2021). Sustain Release Matrix Tablet: An Overview. *Asian Journal of Pharmaceutical Research and Development*, 9(3), 112117.

Mishra, M., Pandey, A. K., Pandey, K., Dixit, S., Zohra, F., Seth, A., & Singh, S. (2021). Exploring the Potential of Nanotechnology in Agriculture: Current Research and Future Prospects. *Composite Materials*, 223-241.

Mitra, S., Lami, M. S., Uddin, T. M., Das, R., Islam, F., Anjum, J., & Emran, T. B. (2022). Prospective multifunctional roles and pharmacological potential of dietary flavonoid narirutin. *Biomedicine & Pharmacotherapy*, 150, 112932.

Mostafavi, E., Soltantabar, P., & Webster, T. J. (2019). Nanotechnology and picotechnology: a new arena for translational medicine. *Biomaterials in Translational Medicine*, 191-212.

Muthuraj, S. (2019). Pharmacognostical, Phytochemical and In Vitro Anti Diabetic Evaluation of Seed Extracts of Casuarina Equisetifolia Linn. *International Conference on Tropical Studies (ICTROPS)*, 213-241.

Napagoda, M., & Witharana, S. (2020). Exploring the Plant Kingdom for Sources of Skincare Cosmeceuticals: From Indigenous Knowledge to the Nanotechnology Era. *Wild Plants,* 426-443.

Nethi, S. K., Das, S., Patra, C. R., & Mukherjee, S. (2019). Recent advances in inorganic nanomaterials for wound-healing applications. *Biomaterials Science*, *7*(7), 26522674.

Nezhad-Mokhtari, P., Javanbakht, S., Asadi, N., Ghorbani, M., Milani, M., Hanifehpour, Y. & Akbarzadeh, A. (2021). Recent advances in honey-based hydrogels for wound healing applications: Towards natural therapeutics. *Journal of Drug Delivery Science and Technology*, 102-389.

Niveditha, T. M. A. (2019). Applications of nanomedicine-Overview. *Journal of Nanotechnology*, *5*(1), 336-338.

Noorbakhsh, S. I., Bonar, E. M., Polinski, R., & Amin, M. S. (2021). Educational Case: Burn Injury Pathophysiology, Classification and Treatment. *Academic Pathology*, *8*-34.

Obeid, M. A., Gany, S. A. S., Gray, A. I., Young, L., Igoli, J. O., & Ferro, V. A. (2020). Niosome-encapsulated balanocarpol: compound isolation, characterisation, and cytotoxicity evaluation against human breast and ovarian cancer cell lines. *Nanotechnology*, 31(19), 195101.

Oloninefa, S. D., Abalaka, M. E., Daniyan, S. Y. & Mann, A. (2018). Comparisons between different crude extract yields of whole plant of *Momordica charantia* and their Antibacterial Susceptibility against Selected Clinical Isolates. *Journal of Microbiology Research*, 3 (1), 61-70.

Omotoso, D. R., Ajeigbe, K. O., Owonikoko, W. M., Okwuonu, U. C., Akinola, A. O., Daramola, O. O., & Bienonwu, E. O. (2019). Role of mucous cell and protein in gastroprotective activity of methanolic extracts of Ageratum conyzoides Linn in rats. *African Journal of Biotechnology*, 18(27), 640-646.

Ovais, M., Khalil, A. T., Islam, N. U., Ahmad, I., Ayaz, M., Saravanan, M., & Mukherjee, S. (2018). Role of plant phytochemicals and microbial enzymes in biosynthesis of metallic nanoparticles. *Applied Microbiology and Biotechnology*, 102, 6799-6814.

Panotopoulos, G. P., & Haidar, Z. S. (2019). Mathematical modeling for pharmaco-kinetic and-dynamic predictions from controlled drug release nanosystems: a comparative parametric study. *Scientifica*, 12, 67-384.

Pashkov, D. M., Guda, A. A., Kirichkov, M. V., Guda, S. A., Martini, A., Soldatov, S. A., & Soldatov, A. V. (2021). Quantitative analysis of the UV–vis spectra for gold nanoparticles powered by supervised machine learning. *The Journal of Physical Chemistry C*, 125(16), 8656-8666.

Patel, J. A., Singh, R. P., Patel, V., & Goswami, S. (2022). Application of mathematical models in drug release kinetics of Lagerstroemia speciosa extract-phospholipid complex. *Research Journal of Pharmacy and Technology*, 15(3), 1257-1262.

Pathania, D., Sharma, M., Kumar, S., Thakur, P., Torino, E., Janas, D., & Thakur, S. (2021). Essential oil derived biosynthesis of metallic nano-particles: Implementations above essence. *Sustainable Materials and Technologies*, 30, 2-45.

Patouna, A., Vardakas, P., Skaperda, Z., Spandidos, D. A., & Kouretas, D. (2023). Evaluation of the antioxidant potency of Greek honey from the Taygetos and Pindos mountains using a combination of cellular and molecular methods. *Molecular Medicine Reports*, 27(2), 1-13.

Patra, J. K., Das, G., Fraceto, L. F., Campos, E. V. R., Rodriguez-Torres, M., AcostaTorres, L. S. & Habtemariam, S. (2018). Nano based drug delivery systems: Recent developments and future prospects. *Journal of Nanobiotechnology*, 16(1), 71.

Peppas, N. A. (2019). Mathematical models for controlled release kinetics. *Medical Applications of Controlled Release*, 169-188.

Permanadewi, I., Kumoro, A. C., Wardhani, D. H., & Aryanti, N. (2019). Modelling of controlled drug release in gastrointestinal tract simulation. *Journal of Physics: Conference Series*, 1295(1), 12063.

Rahman, M. M., Garcia, N., Loh, Y. S., Marks, D. C., Banakh, I., Jagadeesan, P., & Akbarzadeh, S. (2021). A platelet-derived hydrogel improves neovascularisation in full thickness wounds. *Acta Biomaterialia*, 136, 199-209.

Rai, P., Poudyl, A. P., & Das, S. (2019). Pharmaceutical Creams and their use in wound healing: A Review. *Journal of Drug Delivery and Therapeutics*, 9(3), 907-912.

Rana, A., Yadav, K., & Jagadevan, S. (2020). A comprehensive review on green synthesis of nature-inspired metal nanoparticles: Mechanism, application and toxicity. *Journal of Cleaner Production*, 272, 122880.

Rayman, G., Vas, P., Dhatariya, K., Driver, V., Hartemann, A., Londahl, M. (2020). Guidelines on use of interventions to enhance healing of chronic foot ulcers in diabetes. *Diabetes/Metabolism Research and Reviews*, 36, e3283.

Requejo, K. I., Liopo, A. V., Derry, P. J., & Zubarev, E. R. (2019). Improving the shape yield and long-term stability of gold nanoprisms with Poly (Vinylpyrrolidone). *Langmuir*, 35(30), 9777-9784.

Sabourian, P., Tavakolian, M., Yazdani, H., Frounchi, M., Ven, T. G., Maysinger, D., & Kakkar, A. (2020). Stimuli-responsive chitosan as an advantageous platform for efficient delivery of bioactive agents. *Journal of Controlled Release*, 317, 216-231.

Sadat, Z., Farrokhi-Hajiabad, F., Lalebeigi, F., Naderi, N., Gorab, M. G., Cohan, R. A., & Maleki, A. (2022). A comprehensive review on the applications of carbon-based nanostructures in wound healing: from antibacterial aspects to cell growth stimulation. *Biomaterials Science*, 10(24), 6911-6938.

Sadh, P. K., Chawla, P., & Duhan, J. S. (2018). Fermentation approach on phenolic, antioxidants and functional properties of peanut press cake. *Food Bioscience*, 22, 113-120.

Saleh, T. A. (2020). Nanomaterials: Classification, properties, and environmental toxicities. *Environmental Technology & Innovation*, 20, 101067.

Sathyaseelan, L., Thodi, R. C., & Sukumaran, S. T. (2020). Ethnomedicine and Role of Plant Metabolites. *Plant Metabolites: Methods, Applications and Prospects*, 181216.

Sermakkani, M. & Thangapandian, V. (2012). Biological Synthesis of Silver Nanoparticles Using Medicinal Plant (*Cassia italica*) Leaves. *International Journal of Current Research.* 4 (10), 053-058.

Seyed, M. A., & Ayesha, S. (2021). Modern Phytomedicine in Treating Diabetic Foot Ulcer: Progress and Opportunities. *Diabetic Foot Ulcer: An Update*, 281-313.

Shi, Z., Zhou, Y., Fan, T., Lin, Y., Zhang, H., & Mei, L. (2020). Inorganic nano-carriers based smart drug delivery systems for tumor therapy. *Smart Materials in Medicine* 101-281.

Shittu, K.O., Bankole, M T Abdulkareem, A S Abubakre, O. K. & Ubaka, A. U. (2017). Application of gold nanoparticles for improved drug efficiency. *Advances in Natural Sciences: Nanoscience and Nanotechnology,* 8, 1-9.

Shoseyov, O., Kam, D., Ben Shalom, T., Shtein, Z., Vinkler, S., & Posen, Y. (2019). Nanocellulose composite biomaterials in industry and medicine. *Extracellular Sugar-Based Biopolymers Matrices,* 693-784.

Siddique, S., & Chow, J. C. (2020). Application of nanomaterials in biomedical imaging and cancer therapy. *Nanomaterials*, 10(9), 1700.

Soni, M., Mehta, P., Soni, A., & Goswami, G. K. (2018). Green nanoparticles: Synthesis and applications. *Journal. Biotechnology Biochemistry*, 4, 78-83.

Starowicz, M., Lamparski, G., Ostaszyk, A., & Szmatowicz, B. (2021). Quality evaluation of polish honey: On-line survey, sensory study, and consumer acceptance. *Journal of Sensory Studies*, 1, 23-45.

Sullivan, J. V., & Myers, S. (2022). Skin Structure and Function, Wound Healing and Scarring. In *Plastic Surgery Principles and Practice*, 1-14.

Sun, M., Ran, G., Fu, Q., & Xu, W. (2015). The effect of iodide on the synthesis of gold nanoprisms. *Journal of Experimental Nanoscience*, 10(17), 1309-1318.

Talib, S., Ahmed, N., Khan, D., Khan, G. M., & Rehman, A. (2021). Chitosan-chondroitin based artemether loaded nanoparticles for transdermal drug delivery system. *Journal of Drug Delivery Science and Technology*, 61, 102281.

Toledo-Hernandez, E., Pena-Chora, G., Hernandez-Velazquez, V. M., Lormendez, C. C., Toribio-Jimenez, J., Romero-Ramirez, Y., & Leon-Rodriguez, R. (2022). The stingless bees (Hymenoptera: Apidae: Meliponini): a review of the current threats to their survival. *Apidologie*, 53(1), 8.

Tottoli, E. M., Dorati, R., Genta, I., Chiesa, E., Pisani, S., & Conti, B. (2020). Skin wound healing process and new emerging technologies for skin wound care and regeneration. *Pharmaceutics*, 12(8), 735.

Trotta, F., & Mele, A. (2019). Nanomaterials: classification and properties. *Nanosponges Synthesis Application*, 1-26.

Walsh, A. A. (2017). Chemisorption of iodine-125 to gold nanoparticles allows for realtime quantitation and potential use in nanomedicine. *Journal of Nanoparticle Research*, *19*, 1-14.

Wang, W., Lu, K. J., Yu, C. H., Huang, Q. L., & Du, Y. Z. (2019). Nano-drug delivery systems in wound treatment and skin regeneration. *Journal of Nanobiotechnology*, 17(1), 1-15.

Yafout, M., Ousaid, A., Khayati, Y., & El Otmani, I. S. (2021). Gold nanoparticles as a drug delivery system for standard chemotherapeutics: A new lead for targeted pharmacological cancer treatments. *Scientific African*, 11, e00685.

Zanchini, R., Blanc, S., Pippinato, L., Di Vita, G., & Brun, F. (2022). Consumers' attitude towards honey consumption for its health benefits: First insights from an econometric approach. *British Food Journal*, 27, 1017.

Zhang, L., Mazouzi, Y., Salmain, M., Liedberg, B., & Boujday, S. (2020). Antibody-gold nanoparticle bioconjugates for biosensors: synthesis, characterization and selected applications. *Biosensors and Bioelectronics*, 165, 112370.

Zhang, Y., Cai, P., Cheng, G., & Zhang, Y. (2022). A brief review of phenolic compounds identified from plants: Their extraction, analysis, and biological activity. *Natural Product Communications*, 17(1), 1934.

APPENDICES

Appendix A: Au-INCs release kinetic plot for *Staphylococcus*(a) zero order plot (b) first order plot (c) Higuchi plot (d) Kosmeryer-peppas plot)

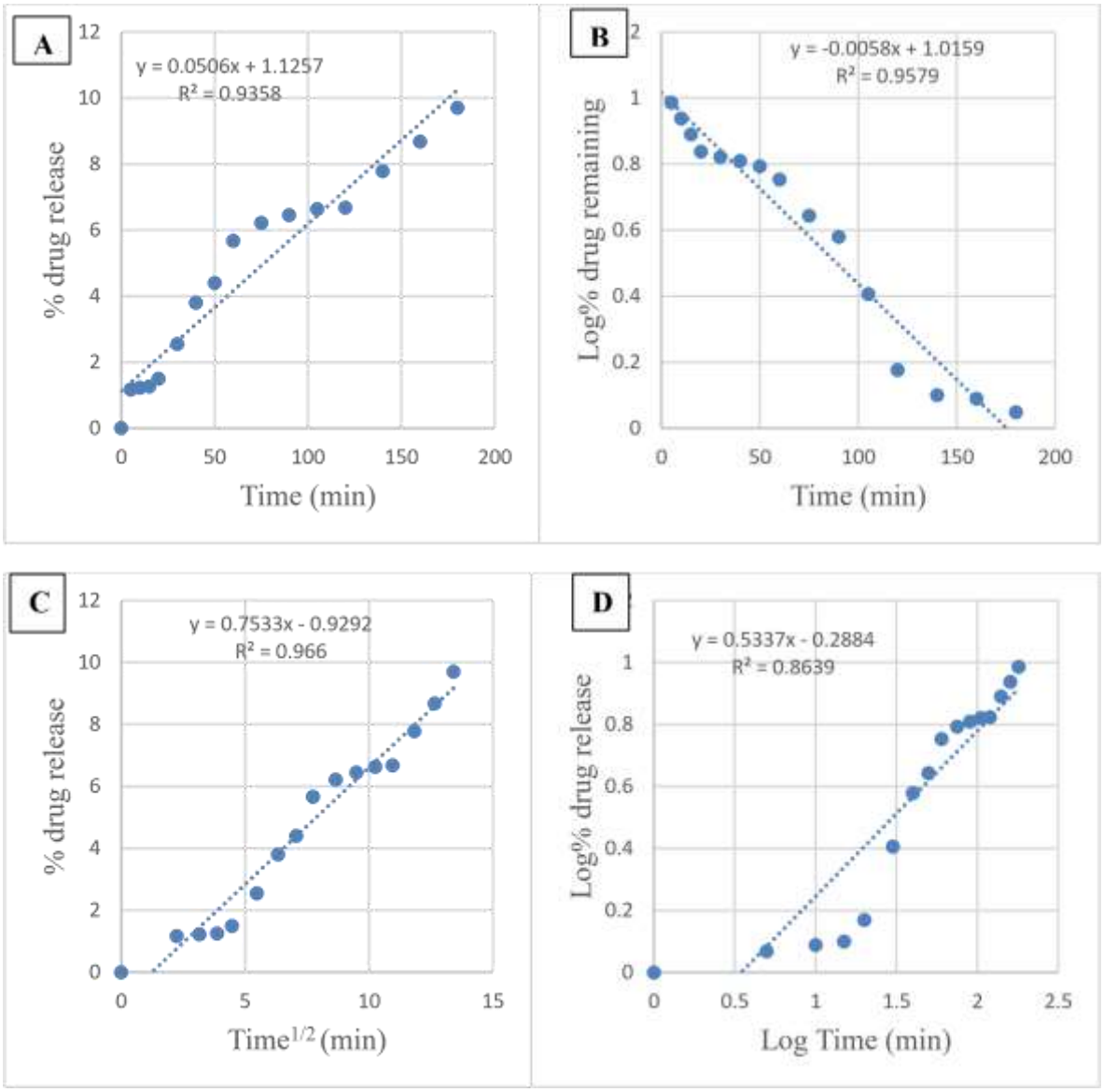

Au-

Appendix B: INCs release kinetic plot for *Pseudomonas*(a) zero order plot (b) first order plot (c) Higuchi plot (d) Kosmeryer-peppas plot)

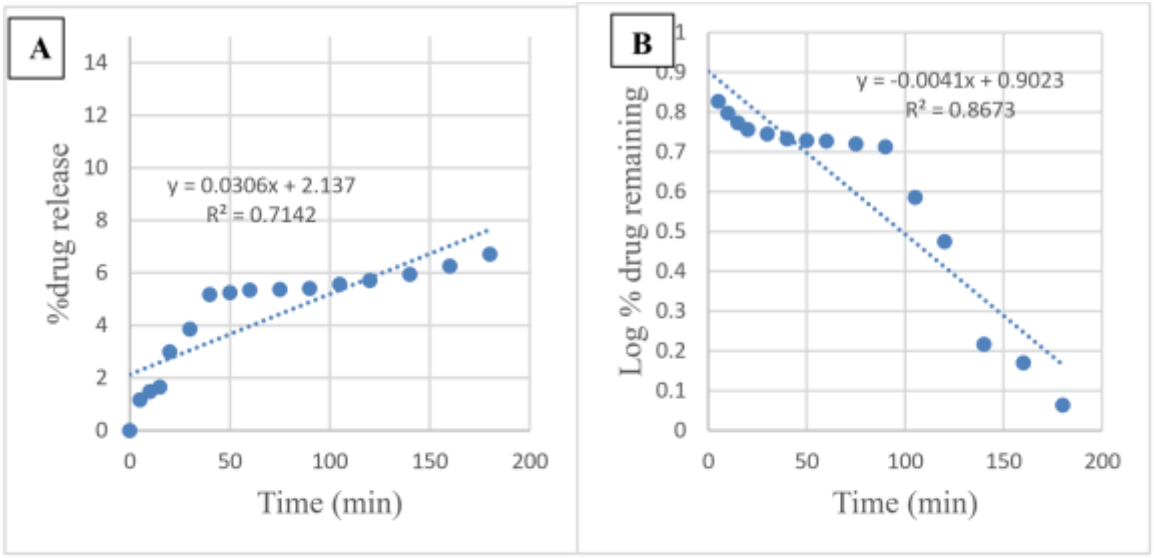

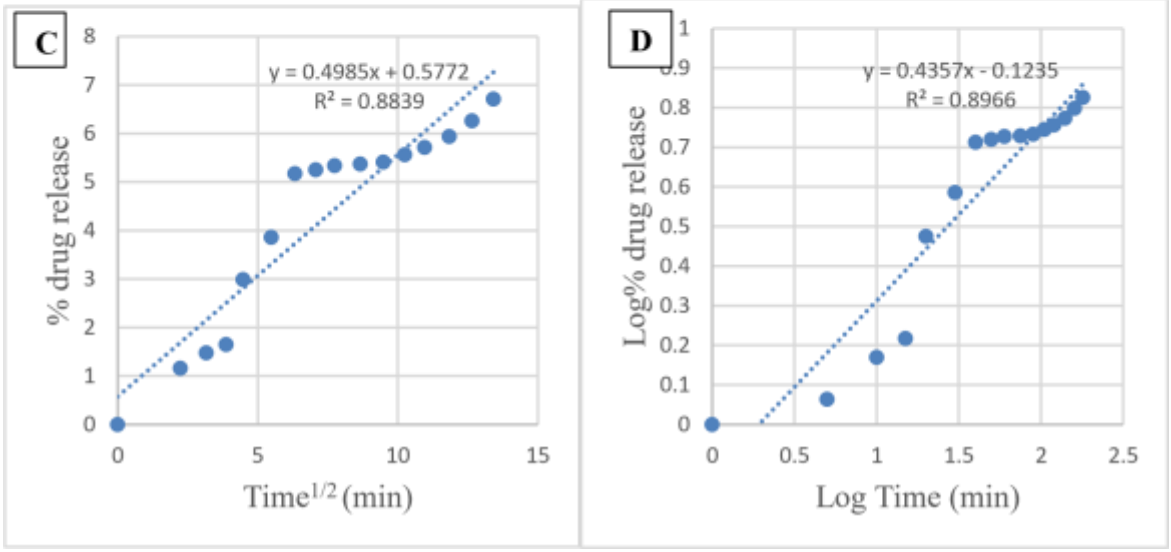

Au-

Appendix C: INCs release kinetic plot for *Escherichia coli*(a) zero order plot (b) first order plot (c) Higuchi plot (d) Kosmeryer-peppas plot)

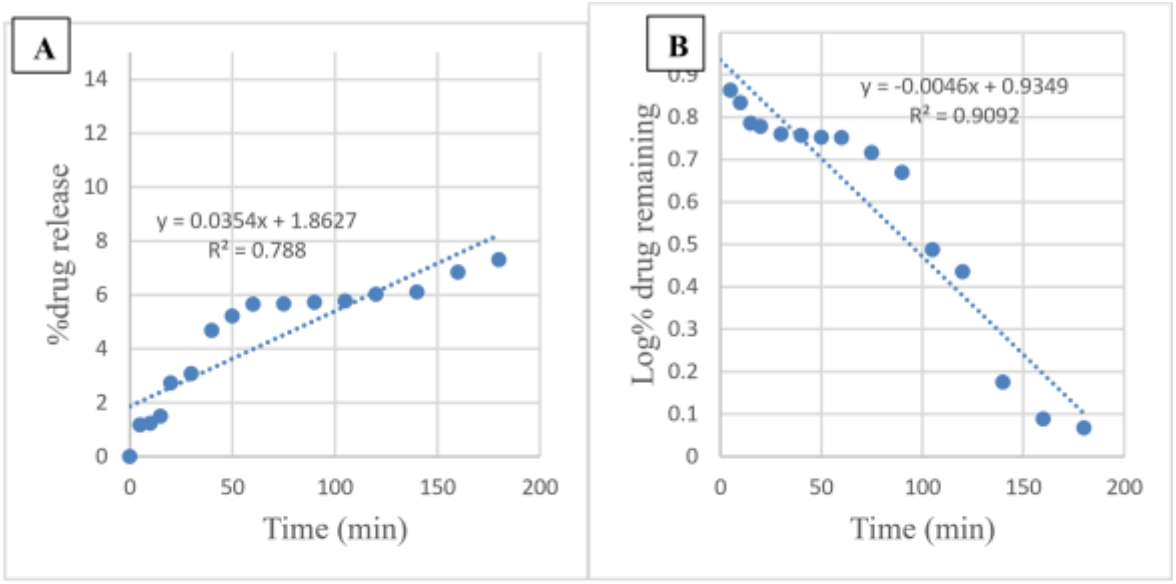

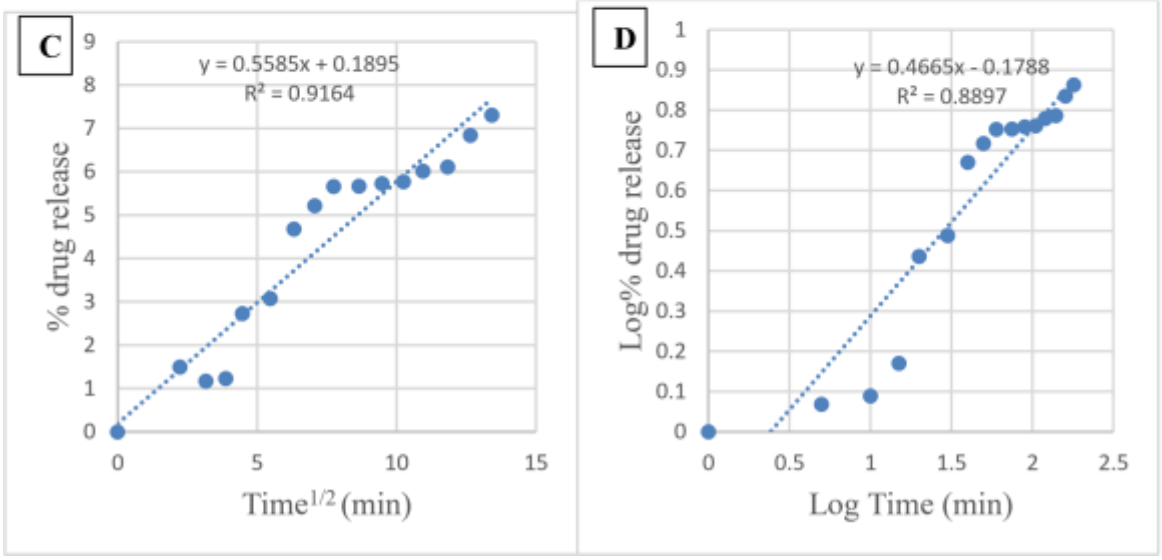

Au-

Appendix D: I/honeyNCs release kinetic plot for *Staphylococcus*((a) zero order plot (b) first order plot (c) Higuchi plot (d) Kosmeryer-peppas plot)

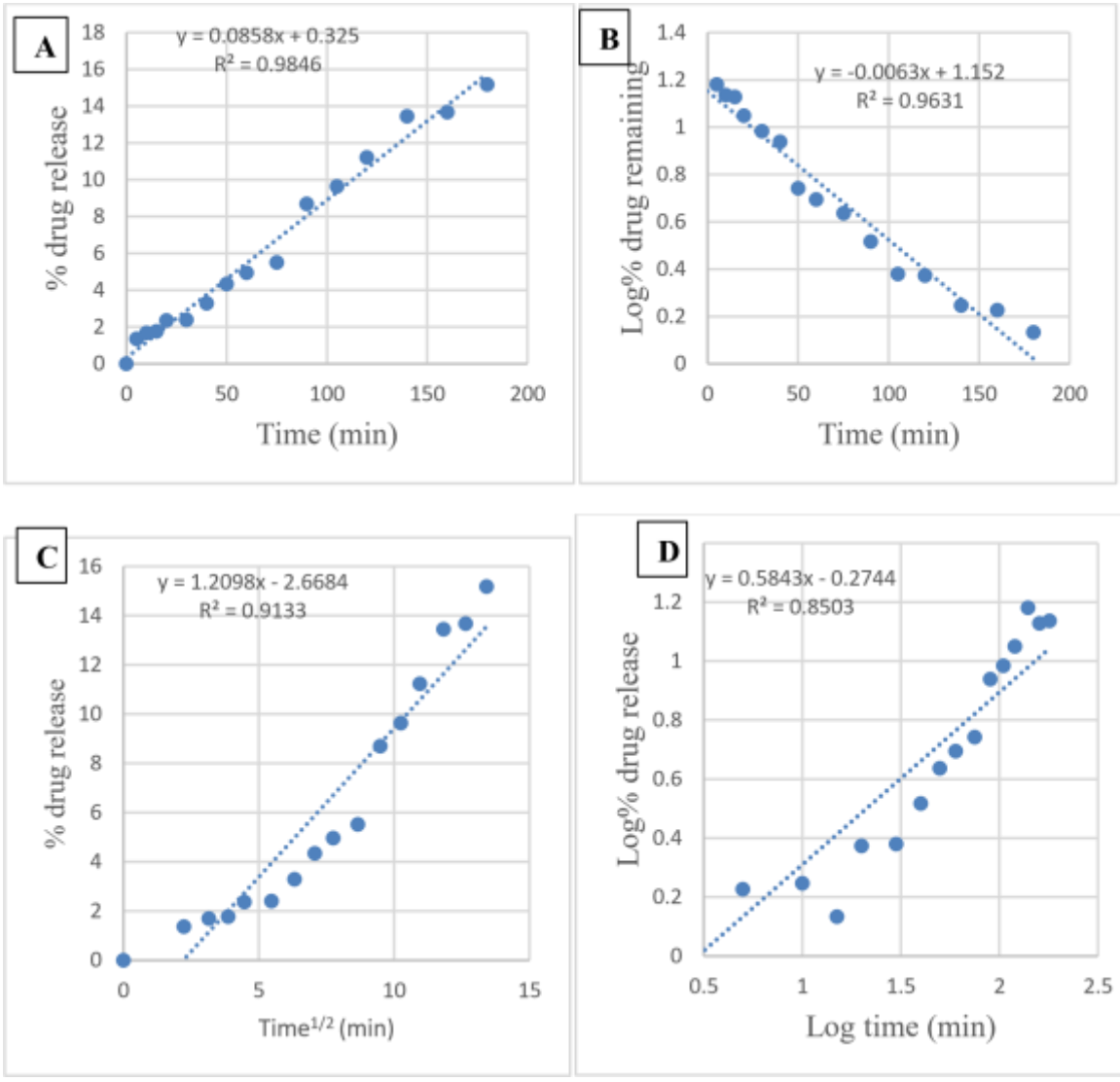

Au-

Appendix E: I/honeyNCs release kinetic plots for *Pseudomonas* (a) zero order plot (b) first order plot (c) Higuchi plot (d) Kosmeryer-peppas plot).

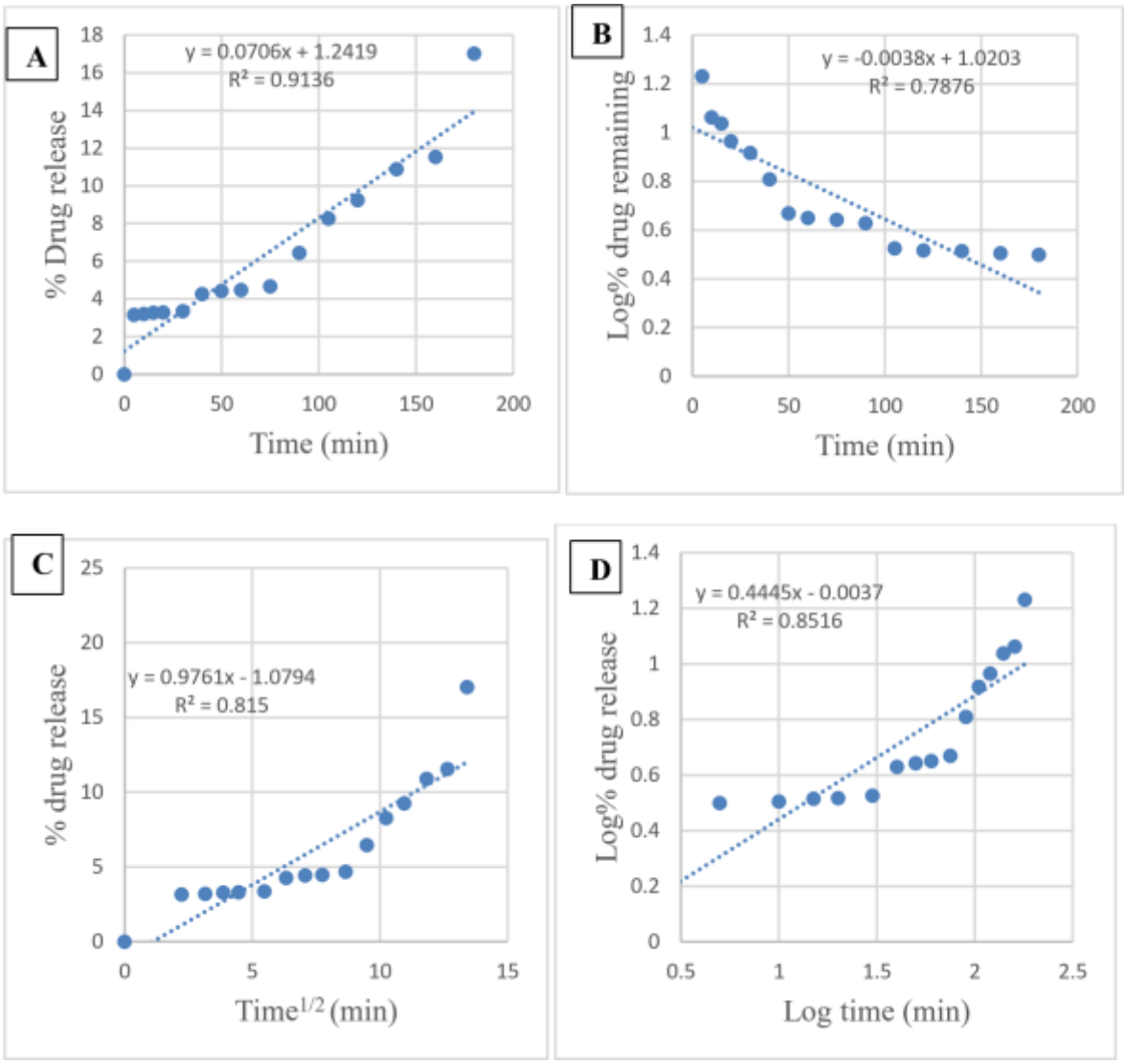

Au-

Appendix F: I/honeyNCs release kinetic plot for *E.coli*((a) zero order plot (b) first order plot (c) Higuchi plot (d) Kosmeryer-peppas plot)